General Disclaimer

One or more of the Following Statements may affect this Document

- This document has been reproduced from the best copy furnished by the organizational source. It is being released in the interest of making available as much information as possible.

- This document may contain data, which exceeds the sheet parameters. It was furnished in this condition by the organizational source and is the best copy available.

- This document may contain tone-on-tone or color graphs, charts and/or pictures, which have been reproduced in black and white.

- This document is paginated as submitted by the original source.

- Portions of this document are not fully legible due to the historical nature of some of the material. However, it is the best reproduction available from the original submission.

JPL Publication No. 83-80

Remote Measurements of Ozone, Water Vapor and Liquid Water Content, and Vertical Profiles of Temperature in the Lower Troposphere

William B. Grant
Bruce L. Gary
Michael S. Shumate

August 22, 1983

Prepared for
California Air Resources Board
Through an Agreement with
National Aeronautics and Space Administration
by
Jet Propulsion Laboratory
California Institute of Technology
Pasadena, California

JPL Publication No. 83-80

Remote Measurements of Ozone, Water Vapor and Liquid Water Content, and Vertical Profiles of Temperature in the Lower Troposphere

William B. Grant
Bruce L. Gary
Michael S. Shumate

August 22, 1983

Prepared for
California Air Resources Board
Through an Agreement with
National Aeronautics and Space Administration
by
Jet Propulsion Laboratory
California Institute of Technology
Pasadena, California

Prepared by the Jet Propulsion Laboratory, California Institute of Technology, for the U.S. Department of Energy through an agreement with the National Aeronautics and Space Administration.

ABSTRACT

Several advanced atmospheric remote sensing systems developed at the Jet Propulsion Laboratory have been demonstrated under various field conditions to determine how useful they would be for general use by the California Air Resources Board and local air quality districts.

One of the instruments reported on is the Laser Absorption Spectrometer (LAS). It has a pair of carbon dioxide lasers with a transmitter and receiver and can be flown in an aircraft to measure the column abundance of such gases as ozone. From an aircraft, it can be used to rapidly survey a large region. The LAS is usually operated from an aircraft, although it can also be used at a fixed location on the ground. Some tests were performed with the LAS to measure ozone over a 2-km horizontal path.

Another system reported on is the Microwave Atmospheric Remote Sensing System (MARS). It is tuned to microwave emissions from water vapor, liquid water, and oxygen molecules (for atmospheric temperature). It can measure water vapor and liquid water in the line-of-sight, and can measure the vertical temperature profile.

FOREWORD

This report on demonstration measurements and feasibility of routine measurement of ozone, water vapor, liquid water content, and temperature profiles in the lower troposphere was prepared for the Research Division of the California Air Resources Board (CARB) by the Laser Monitoring Group of the Atmospheric Sciences Section and the Ground-based Microwave Application Group of the Microwave Observational Systems Section of the Jet Propulsion Laboratory, California Institute of Technology.

We are grateful for the guidance and support furnished by Mr. Charles Unger and Mr. Charles Bennett of the CARB. William Grant and Michael Shumate wrote the sections of the report on the laser measurements of ozone. They gratefully acknowledge the fine technical support of Tom Verbich and Richard Zanteson, the excellent flying of George Cobb and Dick Satterlee, the excellent aircraft ground support of Gary Longworth, the helpful comments of Dave Hinkley and Bob Menzies, and the suggestion of the flight track by Don Lehrman of MRI. Bruce Gary wrote the sections on the microwave measurements of water vapor, liquid water content, and vertical temperature profiles of the lower troposphere.

This work was performed by the Jet Propulsion Laboratory through NASA Task RE-152, Amendment 258, and was sponsored by the California Air Resources Board under Agreement A0-030-31.

TABLE OF CONTENTS

LIST OF FIGURES

LIST OF TABLES

1.0 EXECUTIVE SUMMARY

1.1 INTRODUCTION

In October 1980, the California Air Resources Board (CARB) awarded the Jet Propulsion Laboratory (JPL) a research grant for $30,000 to demonstrate the usefulness of advanced remote sensing techniques under development at JPL for air pollution monitoring. The techniques included the use of CO_2 lasers for the measurement of ozone (O_3) and other gases, and the use of a passive microwave radiometer for the measurement of vertical temperature of the atmosphere, as well as liquid water and water vapor content along the line-of-sight.

The original plan called for JPL to demonstrate the systems in a JPL/NASA program designed to show the usefulness of advanced instrumentation for monitoring air pollution. The systems under development at JPL were to be taken to a local site where a point-monitoring station was established, so that the systems could be compared with the more traditional instruments. Unfortunately, due to the less than expected funding from NASA, that plan could not be implemented.

In 1981, the California Air Resources Board sponsored two other measurement programs in the Los Angeles Basin which could benefit from the type of information that the JPL systems could obtain. One of these programs was the study of the transportation of air pollution from the Los Angeles Basin to the surrounding desert areas. Caltech and Meteorological Research, Inc. (MRI) were the primary contractors in that program. The other program was the measurement of acid fog in the Los Angeles Basin, conducted by Caltech.

The result was that JPL carried out the research project in a series of four unrelated demonstration projects. The first was the use of the JPL Laser Absorption Spectrometer (LAS), an airborne CO_2 laser remote sensing system that measures the ratio of laser radiation backscattered from the Earth's surface, in the Caltech/ MRI transportation study. The LAS was used to measure ozone burdens in the Basin and in the Mojave Desert during several days when the other groups involved in the study were also making field measurements. At the same time, an onboard Dasibi Ozone Monitor was used to measure ozone levels at flight altitude (usually 8,000 ft above ground), and to measure ozone vertical profiles at various points along the flight path.

For the second project, in 1982 the LAS was reconfigured slightly and used in a fixed location on the ground with stationary targets 1-2 km from the LAS. It was used to evaluate its performance on the ground as a long-path monitor of ozone.

The third project involved the microwave passive radiometer, called MARS (Mobile Microwave Atmospheric Remote Sensing System). It was used in June 1982 to measure cloud liquid-water content (LWC) and atmospheric water vapor in Altadena at the same time and place that the Caltech team was measuring acid fog. The frequency used for LWC is 31 GHz, and for water vapor - 22 GHz.

The fourth project involved the MARS van later in 1982 to measure vertical temperature profiles of the atmosphere from a location at Loyola Marymount University (near the Los Angeles International Airport). This site was chosen to permit comparison of MARS profiles with air truth provided by the radiosondes that were launched each day at noon. The frequencies used for temperature correspond to oxygen molecule lines and are at 54.0, 55.3, and 57.5 GHz.

1.2 SUMMARY OF MEASUREMENT RESULTS

1.2.1 LAS Measurements of Ozone Transport

The LAS was flown successfully on July 22, 30, and 31, 1981. It flew twice daily, with one takeoff near 11 am, the other near 3:30 pm. The flight track was from the Burbank Ariport east through the Banning Pass, north to somewhat past the San Bernardino Mountains, then west along the mountain ranges to a location about 20 miles west of Lancaster. The morning flight served primarily to show that the LAS was working properly.

The primary results were that the LAS could measure ozone burdens in a rapid manner over a long flight path. In addition, the urban plume containing large amounts of ozone was measured on both sides of the mountain ranges on each of the three measurement days. On July 22, it was found on both sides of the San Bernardino Mountains. On July 30, it was found in the vicinity of the Cajon Pass. On July 31, it was found on both sides of the San Gabriel Mountains. These results indicate that the mountains do not contain the ozone, and is contrary to the conventional wisdom.

1.2.2 Long-Path Measurement of Ozone

The LAS was used for measurements of ozone over stationary long-paths over a period of several months. It was found that the signal level was about the same as for the airborne case. However, the temperature stability in the trailer in which it was housed during the summer smog season was very poor, so the laser operating parameters changed as the temperature changed. Apparently reliable data was obtained a few times when the temperature in the van did not change much. The temperature stability problem could probably be solved by regulating the temperature of the laser cooling water. Before that could be done, the time and funds ran out.

1.2.3 Measurement of Cloud Liquid Water Content and Atmospheric Water Vapor

The MARS van was used to measure cloud liquid water content (LWC) and atmospheric water vapor in Eaton Canyon (east Altadena) on June 17,21, and 22, 1982. The water vapor content was found to be a fairly constant 2 cm on these dates. During those measurement days, the MARS van measured cloud LWC varying from 0 microns at cloud burnoff to 900 microns just prior to rain. It was found that mist/drizzle occurred between LWC values of from 400 to 900 microns at the Eaton Canyon site. The LWC measurements were conducted in support of the Caltech acid fog study.

1.2.4 Measurements of Atmospheric Temperature Profiles

Measurements of a temperature inversion layer were attempted in the Los Angeles Basin several times without success. The measurements on September 2 and 3 from JPL failed to show the inversion layer because it was below the altitude of JPL. Measurements at Loyola Marymount University on September 23 were marred by radio frequency interference. Measurements on October 1 and 14 were of good quality, but no temperature inversion developed. Rain later in the month, followed by termination of the radiosonde launches at the end of the month, ended the MARS van temperature measurement program for the season.

The response of the MARS van to temperature inversion layers was analyzed theoretically to complete the project. It is shown that inversions at 4,000 ft altitude should be detectable with the MARS system whenever the temperature contrast across the inversion exceeds about 4°C. Inversions at lower altitudes have less stringent temperature constrast thresholds for detection. MARS/radiosonde comparisons show that 1°C inversions at 500 ft altitude are detectable.

2.0 MEASUREMENT OF OZONE TRANSPORT FROM THE LOS ANGELES BASIN

2.1 INTRODUCTION

The laser absorption spectrometer (LAS) is a remote sensing instrument, designed and built for use in aircraft, and has been used since 1977 to measure tropospheric ozone distributions.[2-1 - 2-5] It is an active, nadir-directed instrument that measures the vertical column abundance of ozone between ground-level and the aircraft altitude. The basis of the measurement is differential absorption of a pair of transmitted wavelengths selected to interact with a sharp spectral feature of the ozone ν_3 band near 9.5-μm wavelength. Two grating-tunable waveguide CO_2 lasers provide the transmitted radiation, and two heterodyne receiver channels in the instrument respond to a small portion of the laser radiation, which is backscattered off the earth's surface below the aircraft and propagated back to collecting telescope.

The purpose of the July 1981 California Air Resources Board program was to study the transport of pollution from the Los Angeles Basin to the surrounding desert areas. The program included SF_6 tracer gas releases in the Basin and in some of the mountain passes, as well as measurements of aerosols, ozone and meteorological parameters. Participants in the study included Professor Fred Shair of California Institute of Tchnology, Donald Lehrman and Dr. Ted Smith of Meteorology Research, Inc., Professor James Edinger of UCLA, and Dr James McElroy of the Las Vegas Laboratories of the US-EPA.

This report describes the LAS and the measurement technique used with it for ozone, presents the results of ozone measurements with it and a Dasibi ozone monitor during the July 1981 CARB program, and then discusses the interpretation of the data.

2.2 LASER ABSORPTION SPECTROMETER: INSTRUMENT DESCRIPTION

The design considerations for the LAS instrument were heavily influenced by aircraft environmental factors. The NASA/JPL Beechcraft twin engine airplane was selected to carry the LAS on its first flight series, and the instrument as a consequence was required to operate in a limited space and in a noisy environment. Two slightly modified Hughes Research Laboratory carbon dioxide waveguide lasers were chosen as the transmitters, with compactness and ruggedness being major considerations. The waveguide lasers were tested for amplitude and frequency stability on a shake table, which was operated at a vibration level which would be encountered in the Beechcraft. The laser is a flowing gas type, designed to emit at a 1-W power level on a large number of lines, which can be selectively tuned by tilting a Littrow-mounted grating and adjusting the voltage on a piezoelectric bimorph. The LAS telescope and other optical components were placed on an aluminum honeycomb plate to provide additional vibration damping, and novel mirror mounts were used which have a special clamping feature which can be activated after alignment adjustments are made. A black anodized shroud was fabricated to enclose completely the optics when the instrument is in operation. The optical head, with one cover panel removed, is shown in Figure 2-1.

An optical schematic for the LAS is shown in Figure 2-2. Only one of the two (signal wavelength and reference wavelength) channels is shown, since they are identical. A small portion of the laser output is reflected off the beam split-

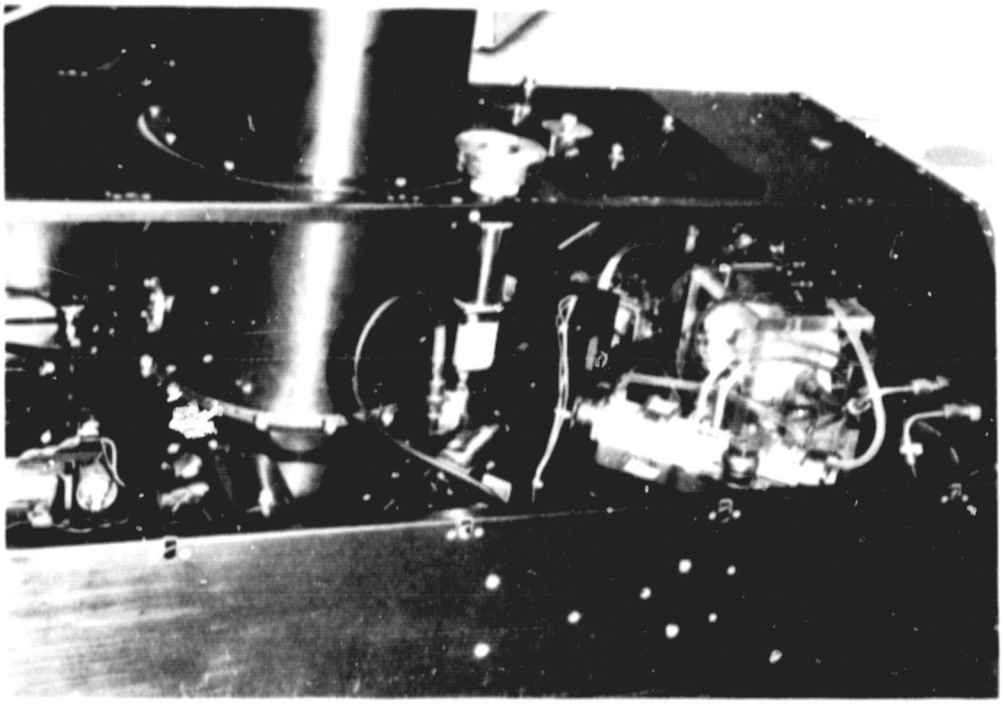

Figure 2-1. LAS Optical Head With One Cover Panel Removed. One of the waveguide CO_2 lasers is in the foreground. Photodetectors are mounted in the bottom-looking nitrogen dewars which are clamped to the telescope tube.

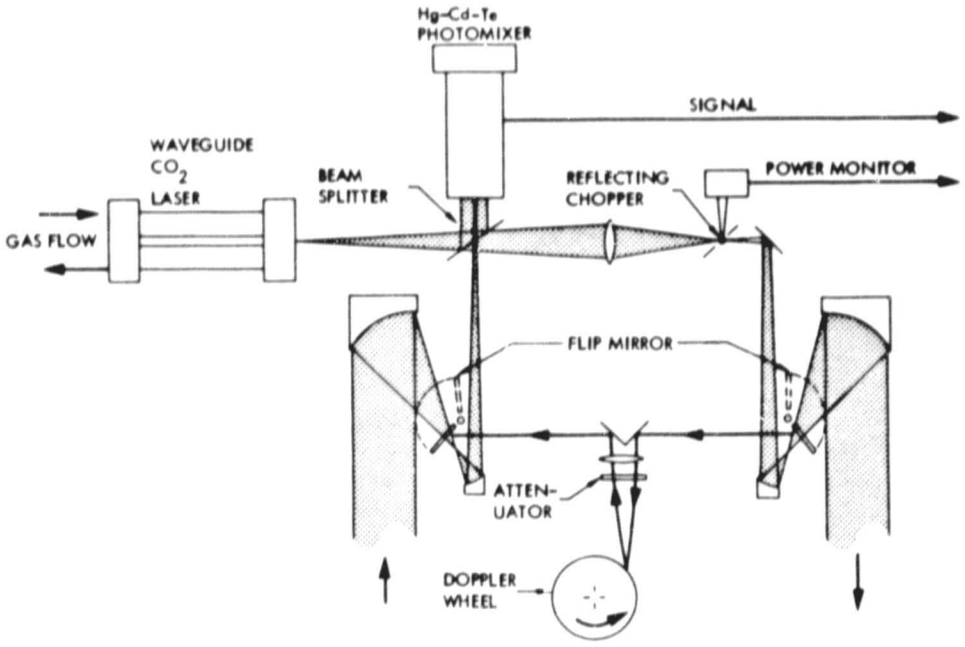

Figure 2-2. LAS Optical Schematic Showing One Channel

ter into the photomixer to serve as a local oscillator. The remainder of the laser radiation is transmitted through a lens which provides optimum coupling to the telescope for a collimated output. At the lens focus, a 1000-Hz tuning fork chopper with a reflective tine modulates the beam with a 50% duty cycle and directs the remainder of the power into a calorimetric power monitor. The received signal is collected by the telescope and focussed onto a liquid-nitrogen-cooled mercury-cadmium-telluride photomixer. A frequency offset between the local oscillator and the received signal is accomplished by tilting the transmit/receive telescope so that the transmitted beam is pointed a few degrees ahead of nadir.

The scattered return radiation is Doppler-shifted a few megahertz by the aircraft's motion. A single telescope, with a 15-cm diameters primary mirror, is divided into four nonoverlaping 5-cm subapertures, two for the transmitted wavelengths and two for the independent heterodyne receivers. An open port is provided in the belly of the airplane to allow the instrument an unobstructed view of the ground.

The receiver electronics block diagram is shown in Figure 2-3 for both channels. The received signals are amplified in a 2-30 MHz passband and then envelope-detected with a square-law detector. Synchronous demodulation at the chopper frequency is followed by an electronic ratiometer and data recording system. Care was taken in the electronics to make certain that both channels had well-matched frequency response and amplitude-response characteristics. During flight operations, the IF amplifier gains were adjusted to limit the signal amplitude into the square-law detectors to keep from driving them into a range of nonsquare-law operation.

The LAS has an internal reference feature. For the system to function properly, the net gain in the two channels must be checked frequently and, ideally, adjusted to be equal. The instrument is placed in the reference mode by energizing a solenoid-actuated motor which inserts a flip mirror into the two transmit beam paths and deflects the transmitted signals to an internal Doppler shifter. The Doppler-shifted radiation is attenuated to the desired level and directed into the receiver optics to produce fixed receiver outputs signals. The gains of the two channels are adjusted to assure that the system is balanced and can thus accurately measure the differntial absorption due to the atmospheric path when the signals are transmitted. During actual flight operations, the LAS is switched to the internal reference mode 10% of the time to check for slow drifts in the system gains.

2.3 LASER ABSORPTION SPECTROMETER: MEASUREMENT TECHNIQUE

The equation used to calculate the concentration of gas (in this case, ozone) in the column below the aircraft is derived from the Beer-Lambert Law for an absorbing medium and takes the form:

$$\rho = \frac{1}{2(\alpha_1-\alpha_2)h} \left[\ell n(\Psi_0\Psi_c/\Psi_g) + \ell n(R_1/R_2)\right] \quad \text{Eq. 2-1}$$

where:

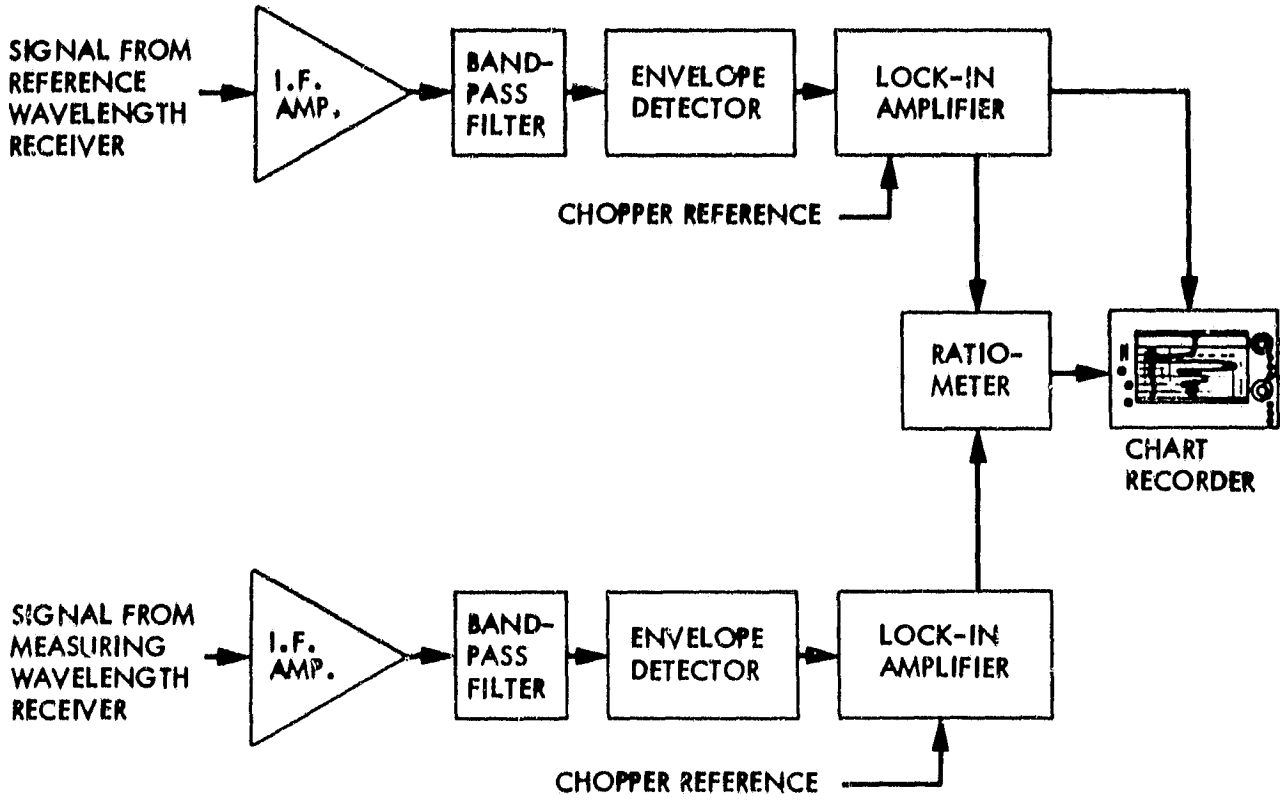

Figure 2-3. Block Diagram of the LAS Electronics and Signal Processing Systems

$[O_3]$ is the average ozone concentration in the column;
is the differential absorption coefficient for ozone, corrected for altitude variations;
h is the air-to-ground distance;
Ψ_g is the ratio of the detected on-line wavelength (P(26)) power to the off-line wavelength (P(24)) power when the instrument is viewing the ground;
Ψ_c is the same ratio when the instrument is viewing an internal doppler wheel;
Ψ_o is the empirically determined value of Ψ_g for the hypothetical case when the atmospheric column contains no ozone;
and $R_{1(2)}$ is the surface reflectance at wavelength 1(2).

Notice that there is a term due to the reflectance of the surface in addition to the term for the ratio of the measured signals. It was determined during the course of flights over a period of several years that the surface reflectance had a spectrally-varying component that was different for different materials. This was studied in the laboratory: for the two laser lines previously employed for ozone measurements, the P(14) line at 9.503 μm and the P(22) line at 9.569 μm, a differential reflectance as high as 20% was found for silica as compared with water.[2-6] This is equivalent to 100 ppb-km of ozone. Because of this, another pair of laser lines was chosen for the measurements reported here: the P(24) line at 9.586 μm and the P(26) line at 9.603 μm. While the differential absorption coefficient for ozone at these wavelengths is down by about a factor of two from that for the earlier wavelength pair, the signal due to the differential spectral reflectance (DSR) of the Earth's surface is down by about a factor of four, so there is a net gain of about a factor of two, assuming that DSR is the largest contribution to the measurment error.

The ozone absorption coefficients have some pressure dependence because the CO_2-laser wavelengths occcur in the wings of the ozone lines.[2-7 - 2-9] For this report, the values of the coefficients at 5500 ft (621 torr) are used. The differential absorption coefficient there for the P(24)-P(26) line pair is 3.87 ± 0.16 atm^{-1} cm^{-1}.

The LAS has to be calibrated fairly frequently - preferrably every 20-30 miles - for several reasons:

- The lasers may change their operating characteristics slightly
- The differential spectral reflectance of the Earth's surface may change significantly
- The vertical profile of ozone may change, thereby altering the averaging required for the column-content measurement

The technique chosen for the calibration is to fly the airplane containing the LAS and a Dasibi ozone monitor in a slow vertical ascending or decending spiral about a point on the flight track (see Figure 2-4). The Dasibi, with a time constant of 30 sec., is used to measure the ozone vertical profile. This profile was then used to calculate Ψ_o in Equation 2-1.

The Dasibi ozone monitor was also used to measure ozone concentrations at the aircraft flight altitude (9,500 or 10,500 ft above mean sea level). The values determined are plotted along with the LAS-determ column-content values.

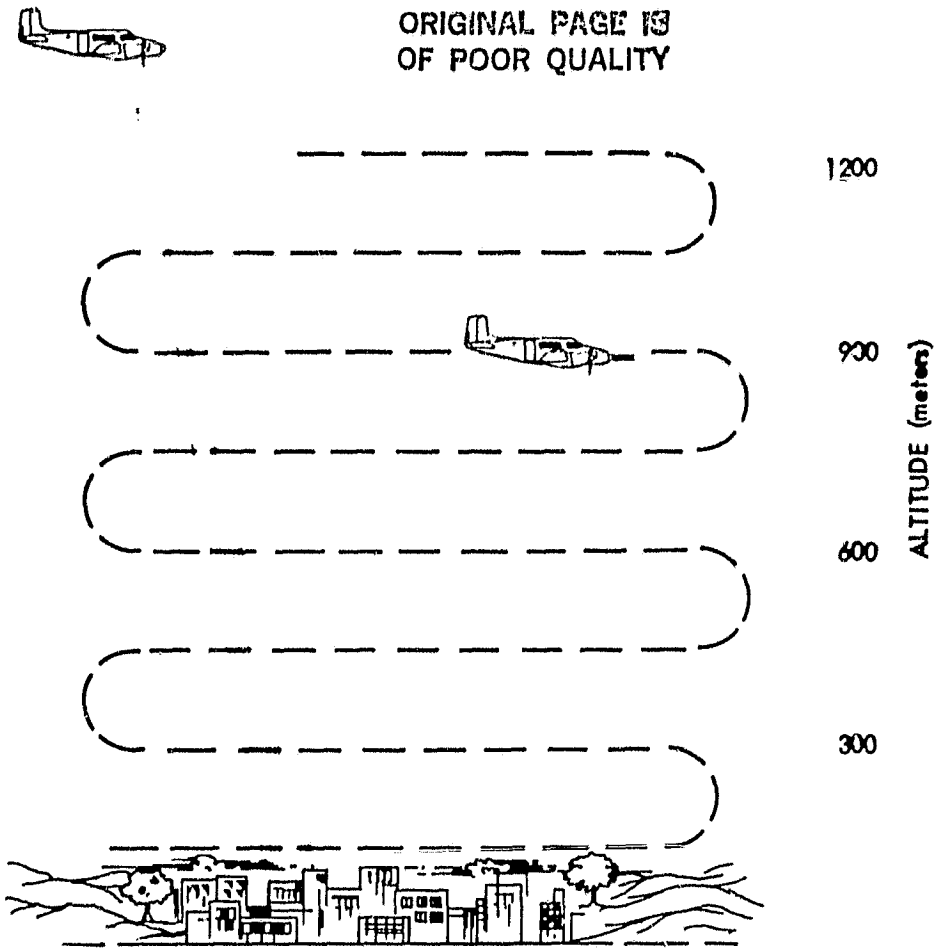

Figure 2-4. Schematic Depiction of the Flight Patterns of the LAS Aircraft (Upper) and in situ Aircraft (Lower) During Calibration Measurements

2.4 MEASUREMENT PROGRAM

The LAS usually flew the same flight track twice a day - one with a late morning PDT departure from the Hollywood-Burbank Airport, the other with a 3:15 pm PDT departure. The flight track is shown in Figure 2-5. There was a vertical profile measurement near the Burbank Airport, a traverse at 9,500 ft. at 120 knots to a location 2 miles north of the Cable Airport, a vertical profile measurement, a traverse at 9,500 ft to just beyond the Banning pass, a vertical profile measurement, a traverse at 9,500 ft to Giant Rock, a traverse usually at 10,500 ft to just west of the Cajon Pass, a vertical profile measurement, a traverse at 10,500 ft to near Lake Hughes, a vertical profile measurement, and then a return to the Hollywood-Burbank Airport. The aircraft altitude was chosen in order to try to be above any ozone that might be transported over the mountains.

The flight schedule for each day that the LAS was flown is given in Table 2-1.

Table 2-1. JPL Flight Schedule

Date	First Flight	Second Flight	Comments
July 9	11:30 a.m. - 1:30 p.m.	4:30 - 5:20 p.m.	No data - gas flow problems
July 14	11:30 a.m. - 1:22 p.m.* 1:45 p.m. - 2:06 p.m.	3:11 - 6:00 p.m.	Poor data-internal calibration problems
July 22	12:49 p.m. - 2:37 p.m.	3:18 - 5:55 p.m.	Good data
July 30	11:50 a.m. - 2:13 p.m.	3:11 - 5:52 p.m.	Good data
July 31	11:10 a.m. - 1:56 p.m.	3:26 - 5:59 p.m.	Good data

*Landed at Fox Field to refuel

The flights each day were arranged to be the same so that useful comparisons could be made. Also, the first flight each day was made to obtain data that could be compared with the afternoon flight.

Grab samples of air were made during many of the spirals. The syringes were given to Professor Fred Shair at Caltech to see whether any SF_6 tracer gas was present from his releases in this study. Some SF_6 was found, and reported elsewhere.

2.5 OZONE MEASUREMENTS

2.5.1 Vertical Profiles Using an On-Board Dasibi Ozone Monitor

The spirals served two functions: one was to provide data on the column content of ozone for calibration of the LAS; the other was to provide information on the

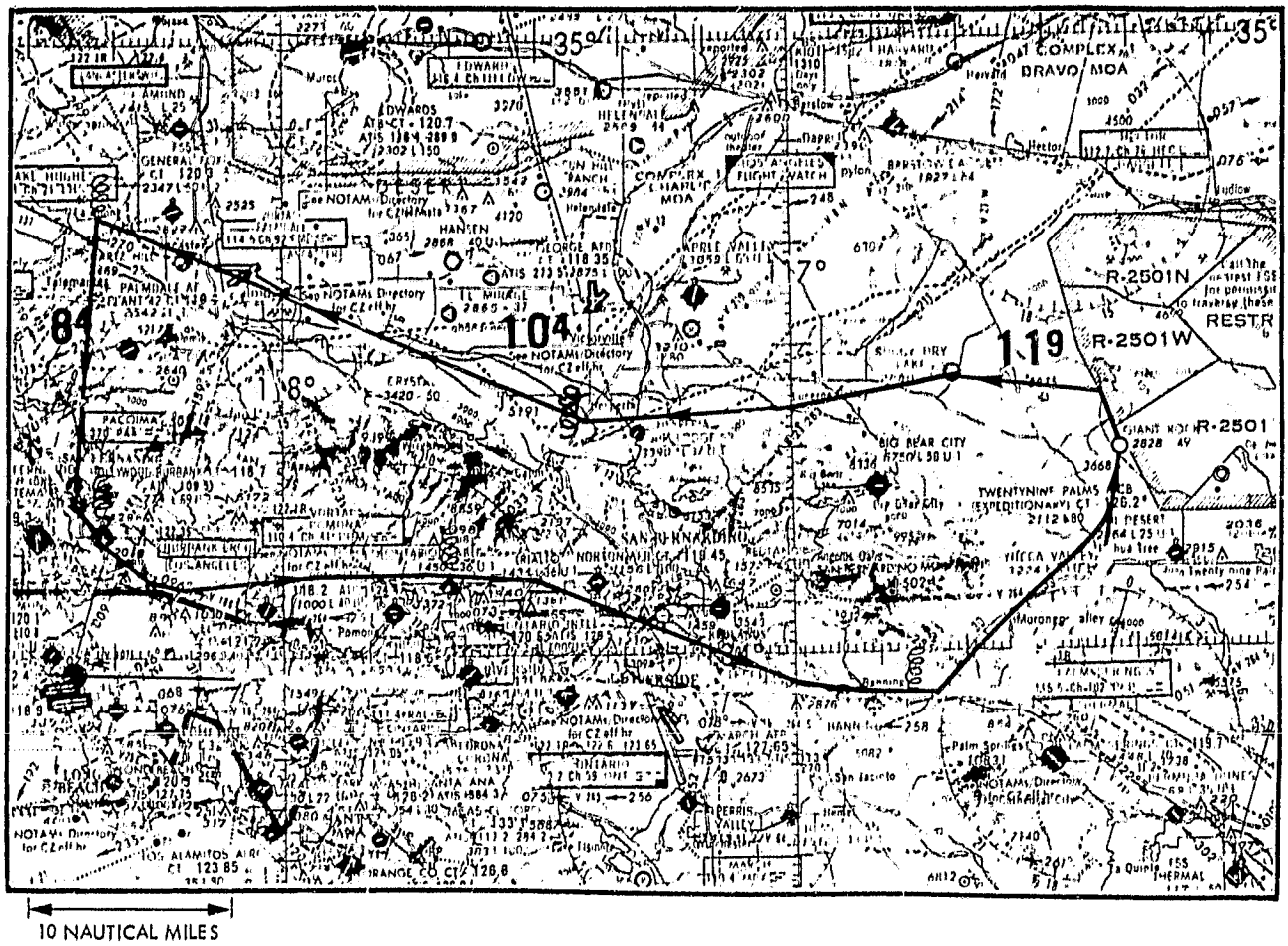

Figure 2-5. Flight Track for the LAS and Dasibi Measurements of Ozone

vertical profile of ozone.

The ozone profile data are shown in Figures 2-6 to 2-13 for July 14, 22, 30, and 31. Several general observations can be made about the data. One is that the mixing depth within the Los Angeles Basin can usually be determined from the profiles, but it is less well defined in the desert because there was often a uniform ozone concentration up to 10,500 ft with higher concentrations in the afternoon.

Another observation is that large regions have similar ozone concentrations and mixing heights. If the mixing height in L.A. Basin were below about 3,000 ft., the Basin appeared to be isolated from the desert. If the mixing height was above that elevation, the air masses appeared to be somewhat linked.

An interesting feature was noticed on the second flight of July 22 -- a second peak in the ozone concentration (see Figure 2-9.) It was near 6,000 ft, had a thickness of about 500 ft, and appeared both in the San Gabriel Valley and in the desert. There are hints of this in some of the other data (e.g., Figure 2-13). From the aircraft, layers of aerosols could occasionally be seen at two or three different heights.

Another interesting feature is that the ozone concentrations often tended to be higher near the top of the mixed layer than near the ground. The effect is especially pronounced for the Burbank Airport, although during the approach from the north, the air directly above the airport was not being sampled. The increases in ozone at the top of the mixing layer are expected - primarily because scavenging gases, such as NO, are more prevalent near the ground, but also because there is more solar radiation at the top.

It is interesting to compare the ozone profiles for given locations for two flights of a given day. At the Cajon Pass, for example, the concentration during the second flight was higher by 20 to 40 ppb above the mixing height. At the Banning Pass, however, the concentration above the mixing height was lower during the second flight of each day.

The region west of the Palmdale Airport usually had less ozone than the Cajon Pass area did in the late afternoon.

2.5.2 Traverses Using the LAS

Ozone was measured in the San Gabriel Valley in order to have some idea of how much ozone was in the Basin that might be transported out to the desert regions. These results are shown in Figures 2-14 to 2-18 for July 22, 30 and 31. Usually, only a few measurements could be made before reaching the Cable Airport because the system was still warming up, and because frequent radio communications to air traffic controllers were required due to air traffic congestion. The radio frequencies used for transmission from the plane interferred with the heterodyne receiver in the LAS.

The vertical column content values were used to provide the calibration constant for the LAS data. As discussed earlier, the LAS is subject to several error sources that could slightly change the calibration constant, Ψ_0.

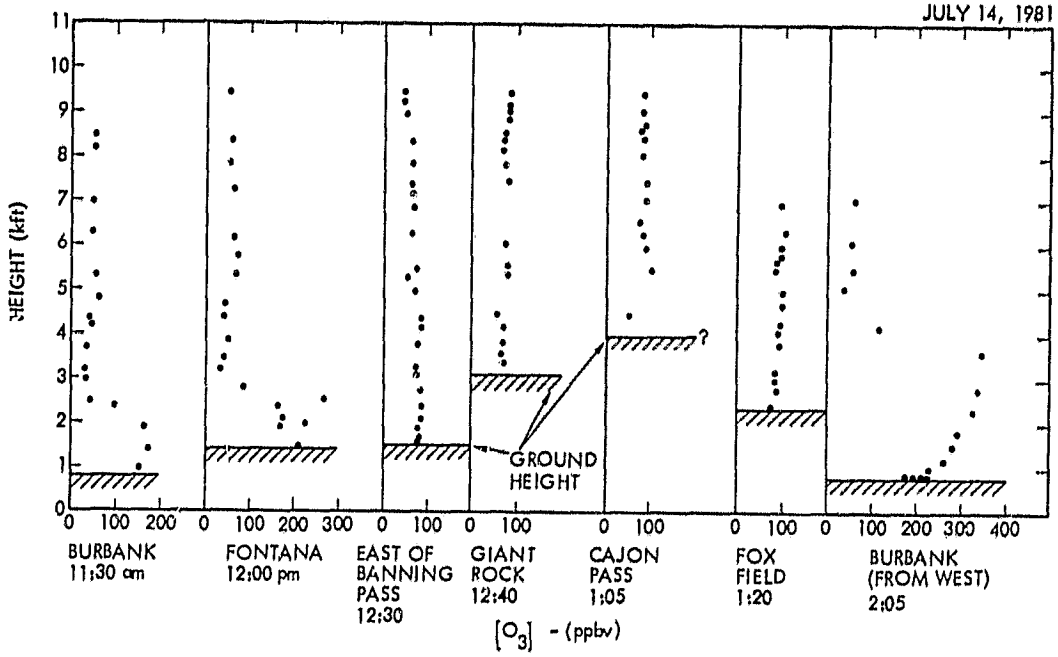

Figure 2-6. Ozone Vertical Profiles Obtained with the Dasibi Ozone Monitor for July 14, 1981 on the First Flight

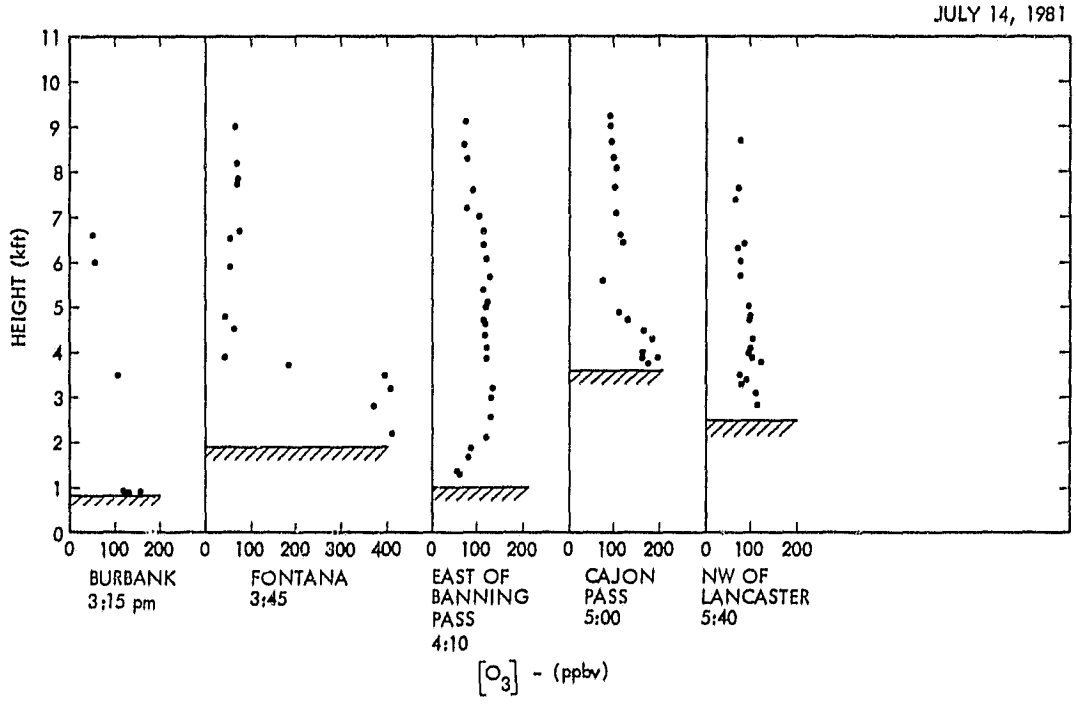

Figure 2-7. Ozone Vertical Profiles as in Figure 2-6 but for the Second Flight on July 14

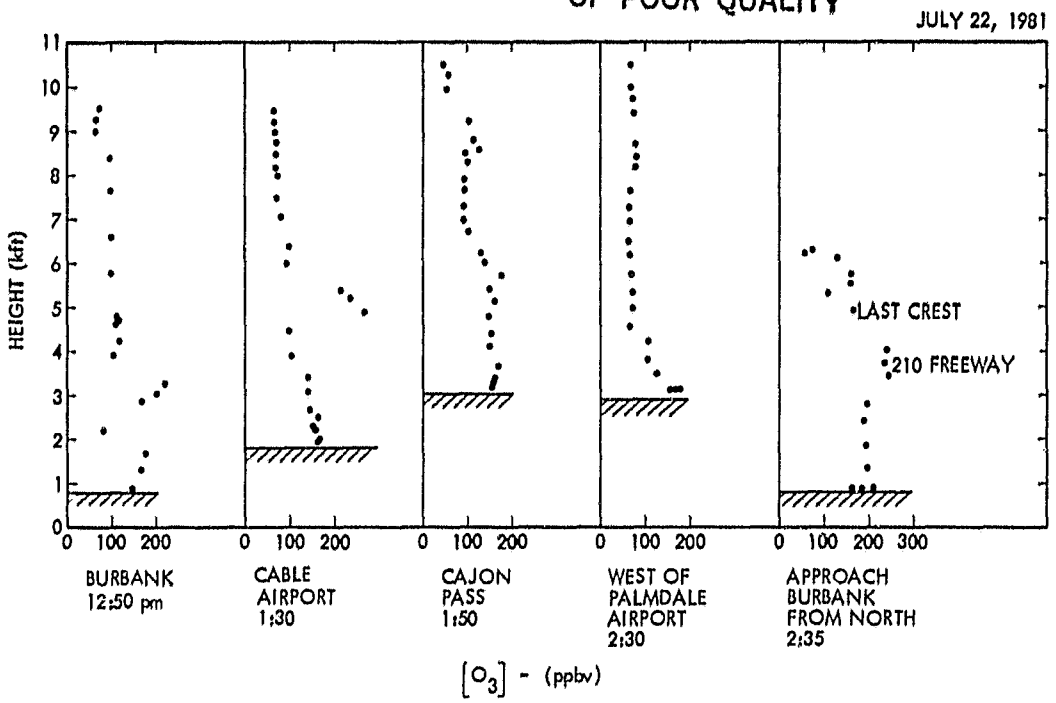

Figure 2-8. Ozone Vertical Profiles for the First Flight of July 22, 1981

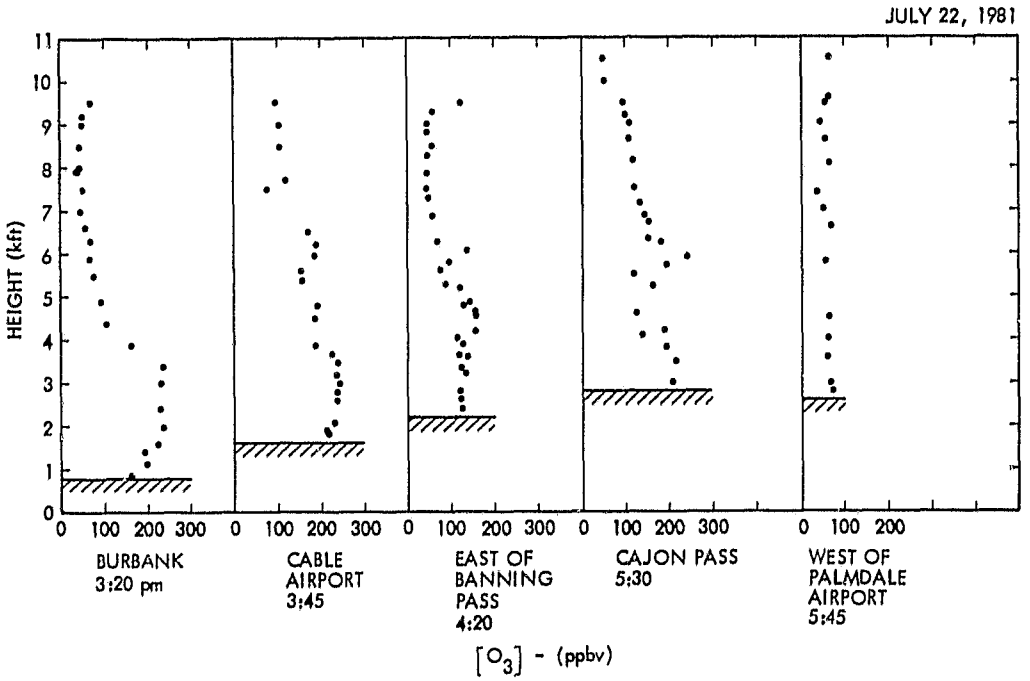

Figure 2-9. Ozone Vertical Profiles for the Second Flight of July 22, 1981

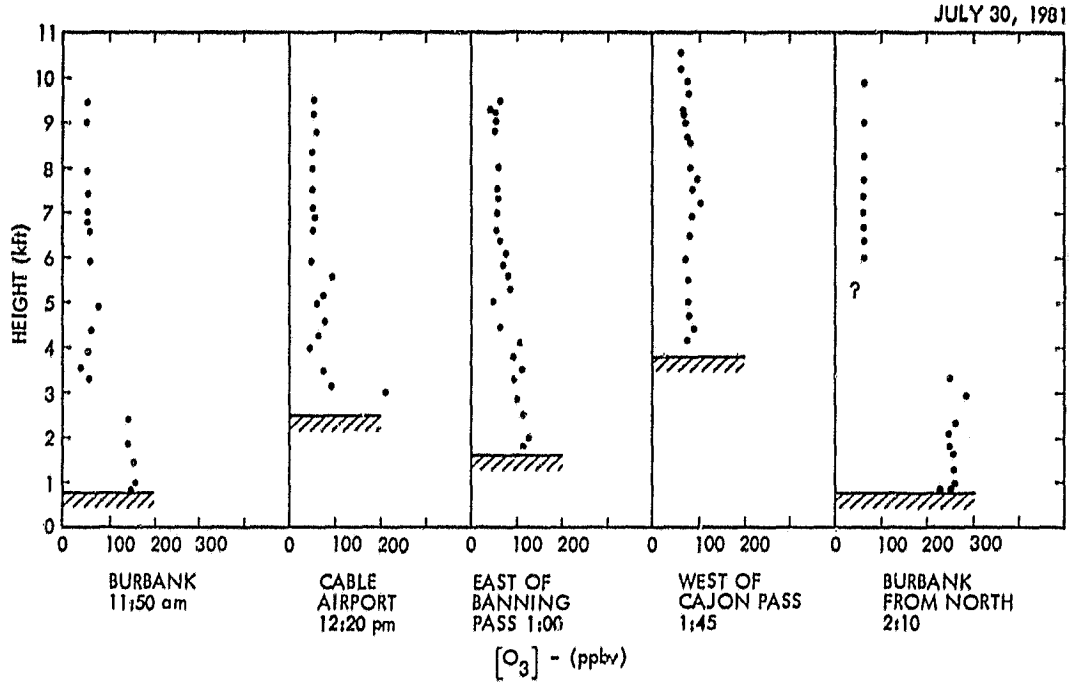

Figure 2-10. Ozone Vertical Profiles for the First Flight of July 30, 1981

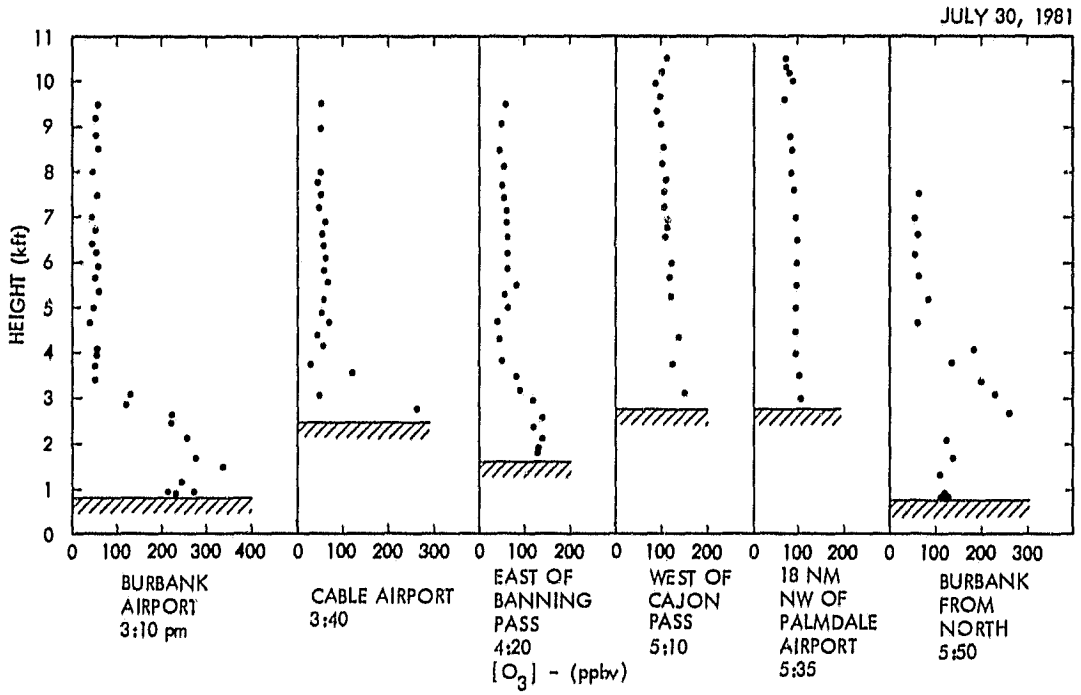

Figure 2-11. Ozone Vertical Profiles for the Second Flight of July 30, 1981

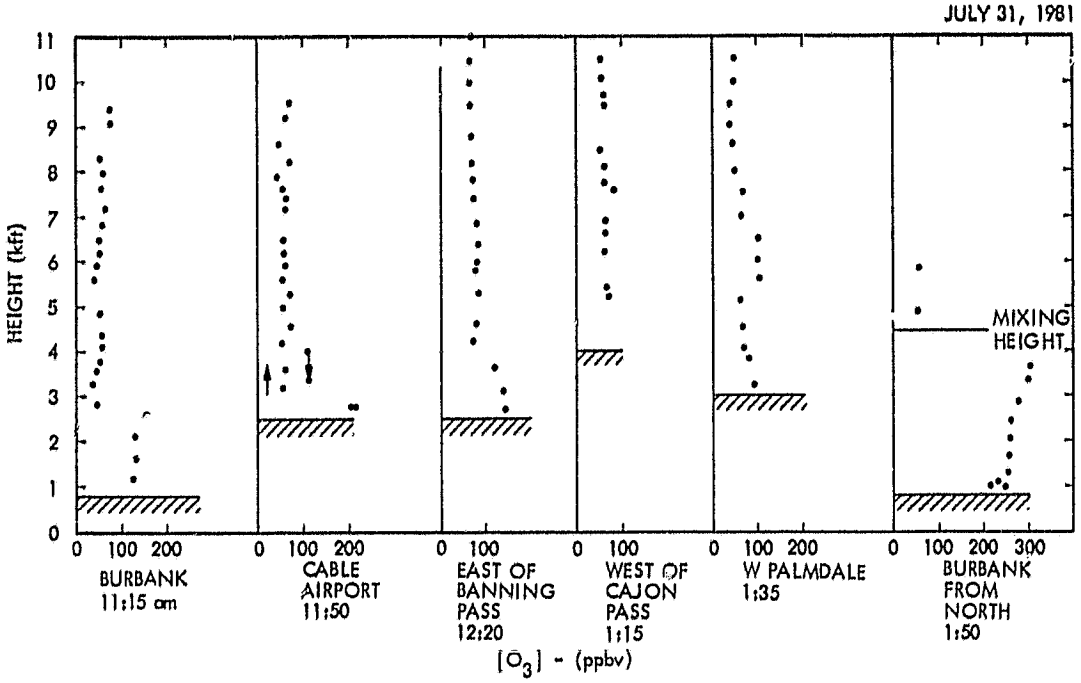

Figure 2-12. Ozone Vertical Profiles for the First Flight of July 31, 1981

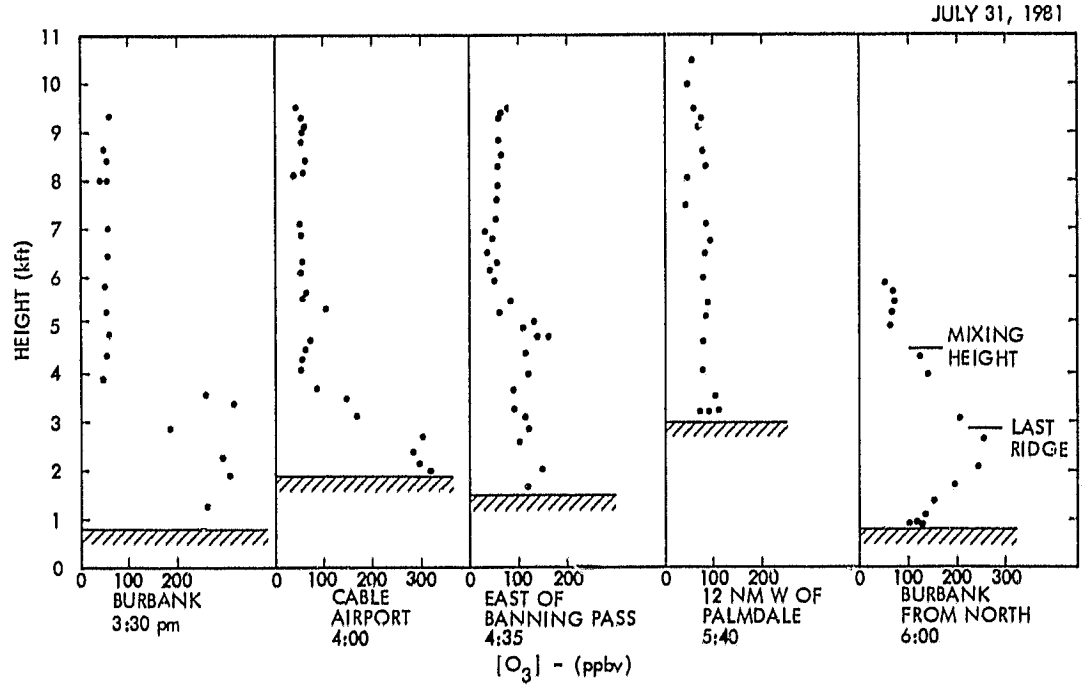

Figure 2-13. Ozone Vertical Profiles for the Second Flight of July 31, 1981

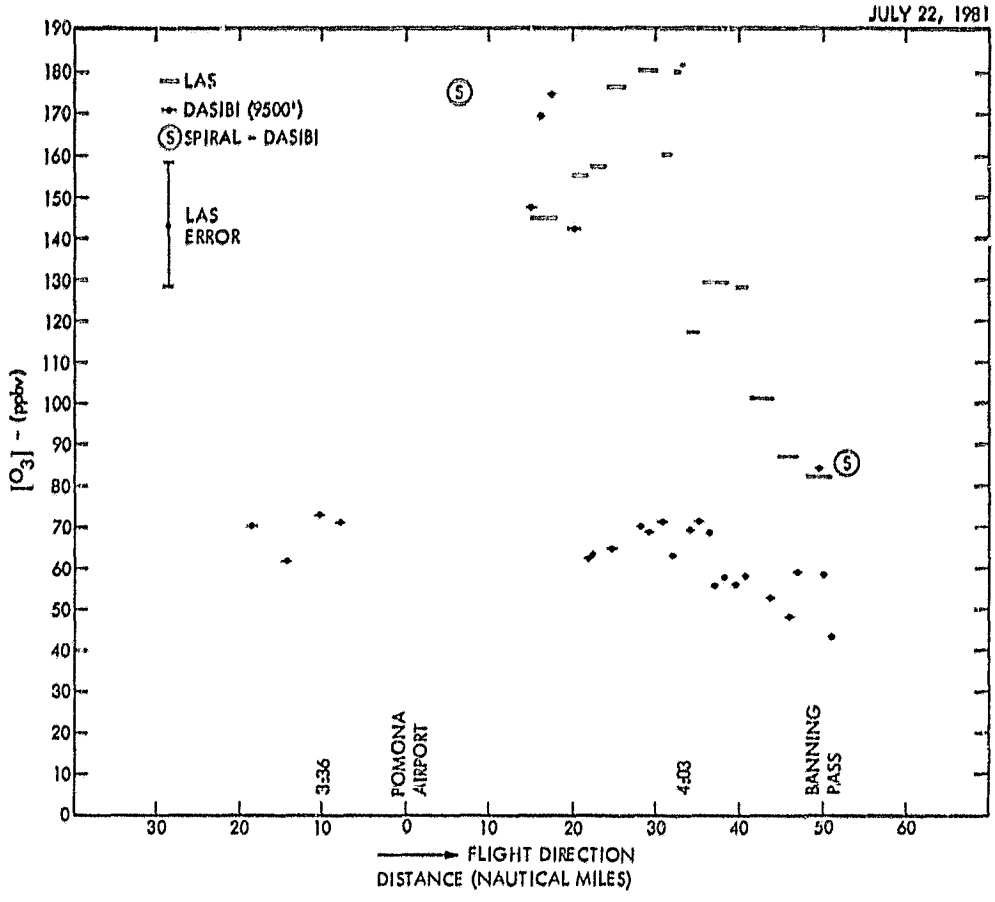

Figure 2-14. Ozone Measured in the San Gabriel Valley During the Second Flight of July 22, 1981. Lines indicate values measured with the LAS; lines with dots indicate values measured with the Dasibi Ozone Monitor at 9500 ft; S indicates values measured during a vertical ascent or descent.

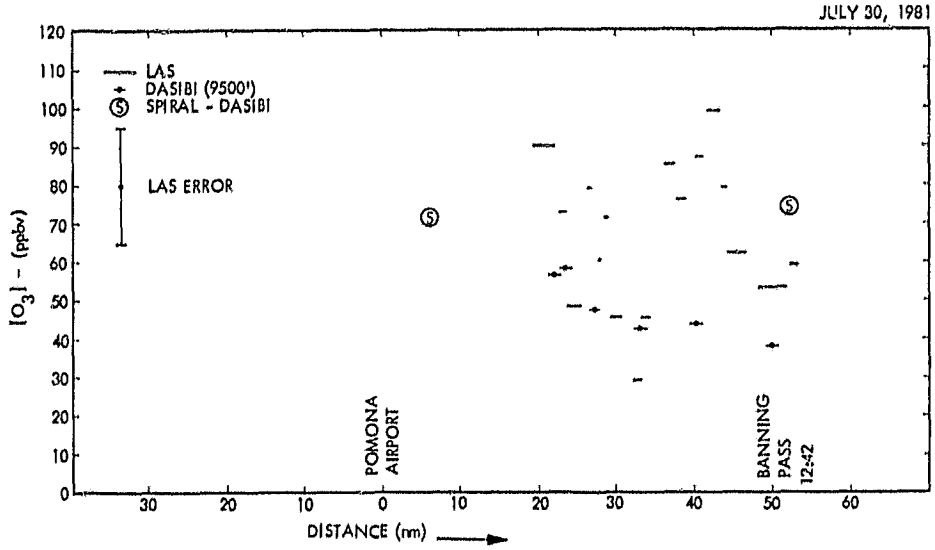

Figure 2-15. Ozone Measured in the San Gabriel Valley During the First Flight of July 30, 1981

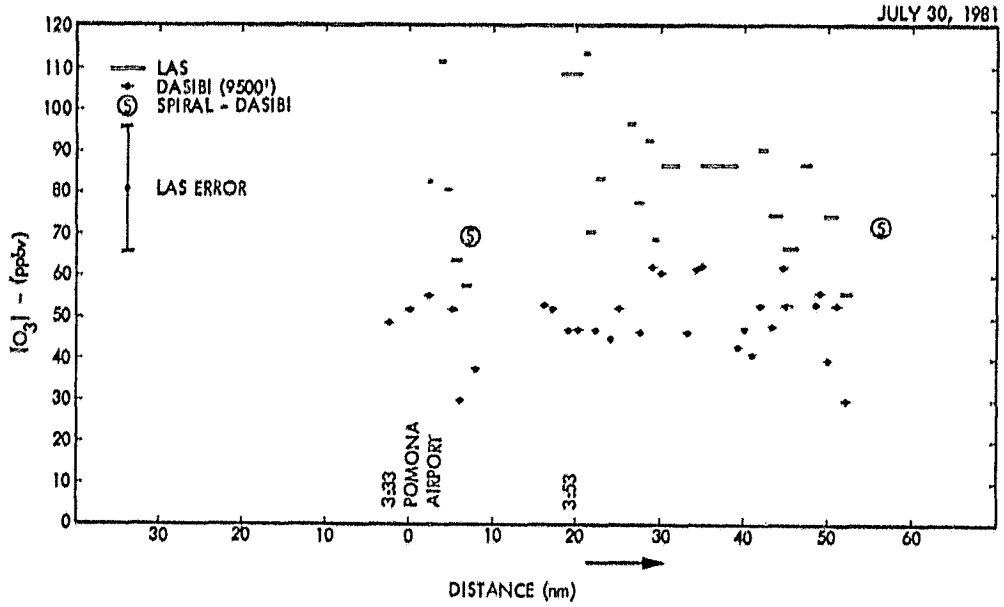

Figure 2-16. Ozone Measured in the San Gabriel Valley During the Second Flight of July 30, 1981

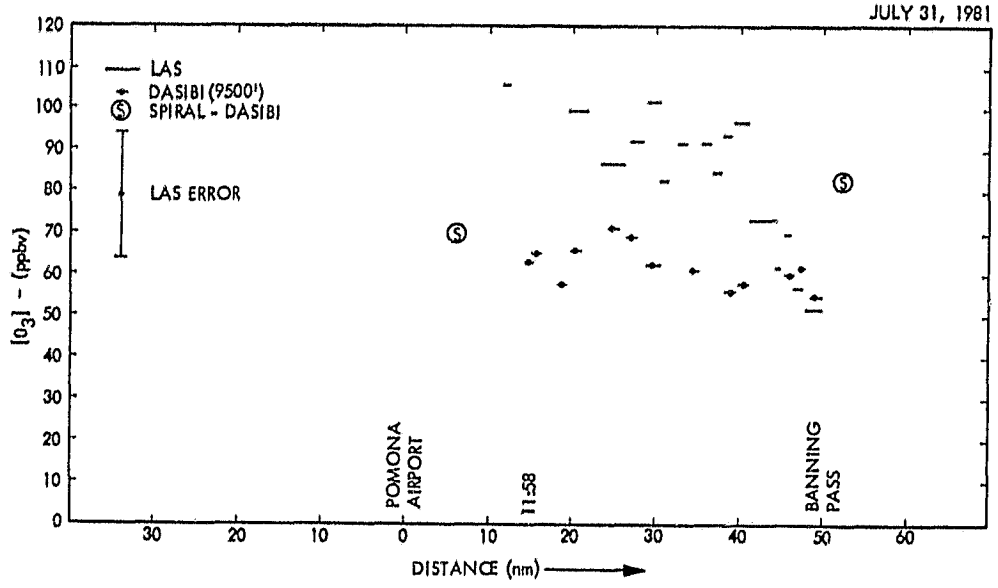

Figure 2-17. Ozone Measured in the San Gabriel Valley During the First Flight of July 31, 1981

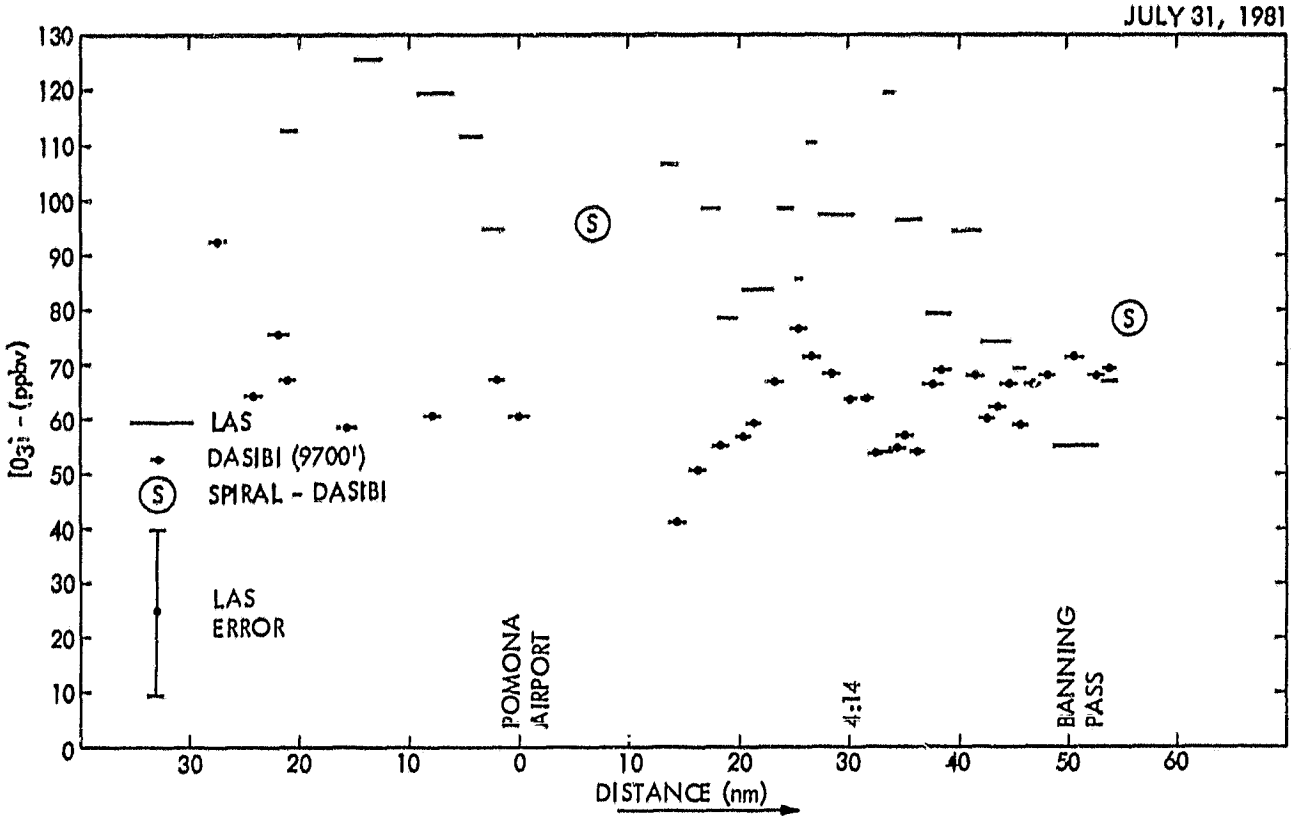

Figure 2-18. Ozone Measured in the San Gabriel Valley During the Second Flight of July 31, 1981

The second flight of July 22 (Figure 2-14) shows a strong ozone peak 30 nautical miles (nm) east of the Pomona Airport using the LAS, and 17 nm east using the Dasibi. The Dasibi vertical profile data (Figure 2-9) substantiate this.

The data from the second flight of July 31, Figure 2-18, indicate that the ozone concentration peak is somewhat west of the Pomona Airport.

The ozone data from the desert between Banning Pass and Giant Rock were not analyzed because inadequate position references were kept and there were no apparent ozone plumes.

The ozone data from the desert north of the San Gabriel Mountains are shown in Figures 2-19 to 2-24 for July 22, 30, and 31.

The data of July 22 show that the ozone concentration is higher to the east of Cajon Pass than to the west. The data of the second flight are consistent with that of the second flight in the San Gabriel Valley. Thirty nautical miles east of Pomona, where the ozone peak occurs, is directly south of the 44 nm spot on Figure 2-20. The two sets of data from the second flight indicate that the ozone might have been transported over the mountains east of the Cajon Pass, in addition to possibly through the pass. The high ozone concentration at 10,500 ft from 55 to 75 miles east of the Palmdale Airport is consistent with this hypothesis. Information on wind velocities would be required to further substantiate this.

The data of July 30 clearly show ozone transport through the Cajon Pass in a north to northwest direction. It is slightly evident at 1:48 p.m., and very evident at 4:58 p.m. The high ozone concentration at 10,500 feet is unusual. The ozone inside the San Gabriel Valley was rather uniformly distributed at both times, and the mixing depth was around 3,000 ft. The Cajon Pass has an elevation below 3,000 ft through most of its length. The mountains to the west as far as the Palmdale Airport are around 7,000 ft above sea level to as high as 10,064 ft to the east; they are around 6,000 ft near the pass to 11,502 ft just north of the Banning Pass. Thus, it is reasonable to expect the ozone to be funnelled through Cajon Pass.

The data of July 31 gave the most interesting observation - the ozone apparently crossed over the mountain ridge west of the Cajon Pass around 5 p.m. As the aircraft approached the pass from the east, the air near the pass was relatively clear. However, a few miles to the west was a large whitish aerosol cloud, apparently smog, with low visibility through it. The customary spiral near the Cajon pass was omitted in favor of obtaining an uninterrupted flight track. The ozone data in the San Gabriel Valley indicate that the ozone concentration was higher west of the Cajon Pass than east of it. The ozone vertical profiles (Figure 2-13) indicate strong mixing up to 3,700 ft in the Los Angeles Basin, with weaker mixing up to about 5,000 ft.

When the aircraft was flying near the top of the mixing layer in the San Gabriel Valley, it was usually noticed that the smog level was higher to the north than to the south, as if smog were being transported up and over the mountains. This is also borne out in the ozone profile data near the Burbank Airport, where the mixing depth measured during the east take-off is lower than during the later approach from the north over a mountain range.

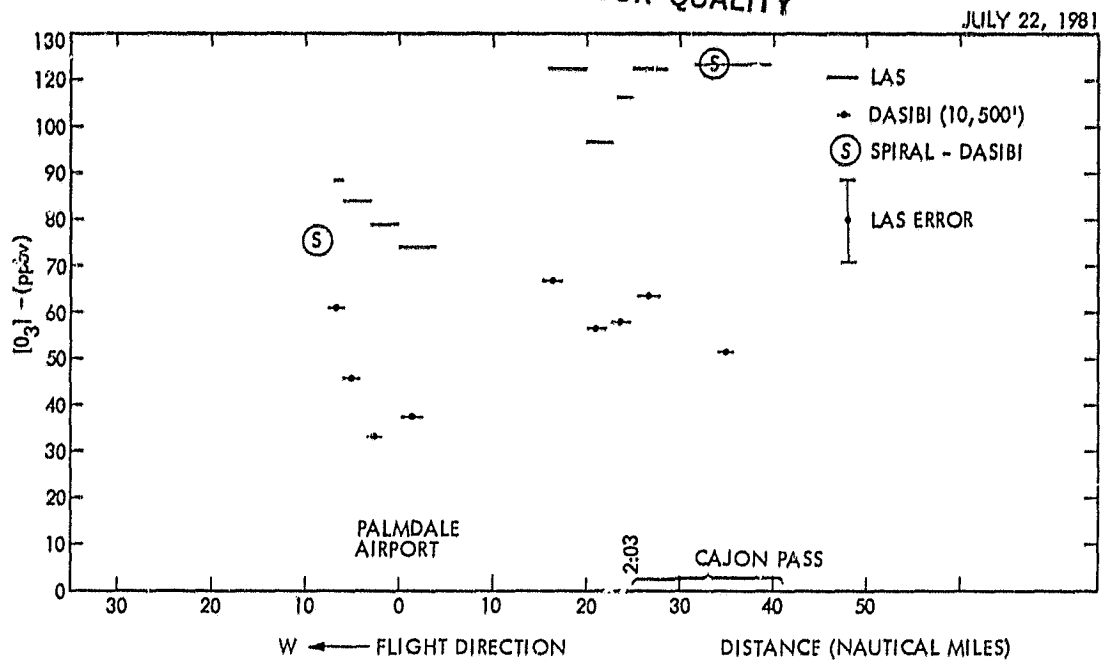

Figure 2-19. Ozone Measured in the Desert North of the San Gabriel and San Bernardino Mountains During the First Flight of July 22, 1981

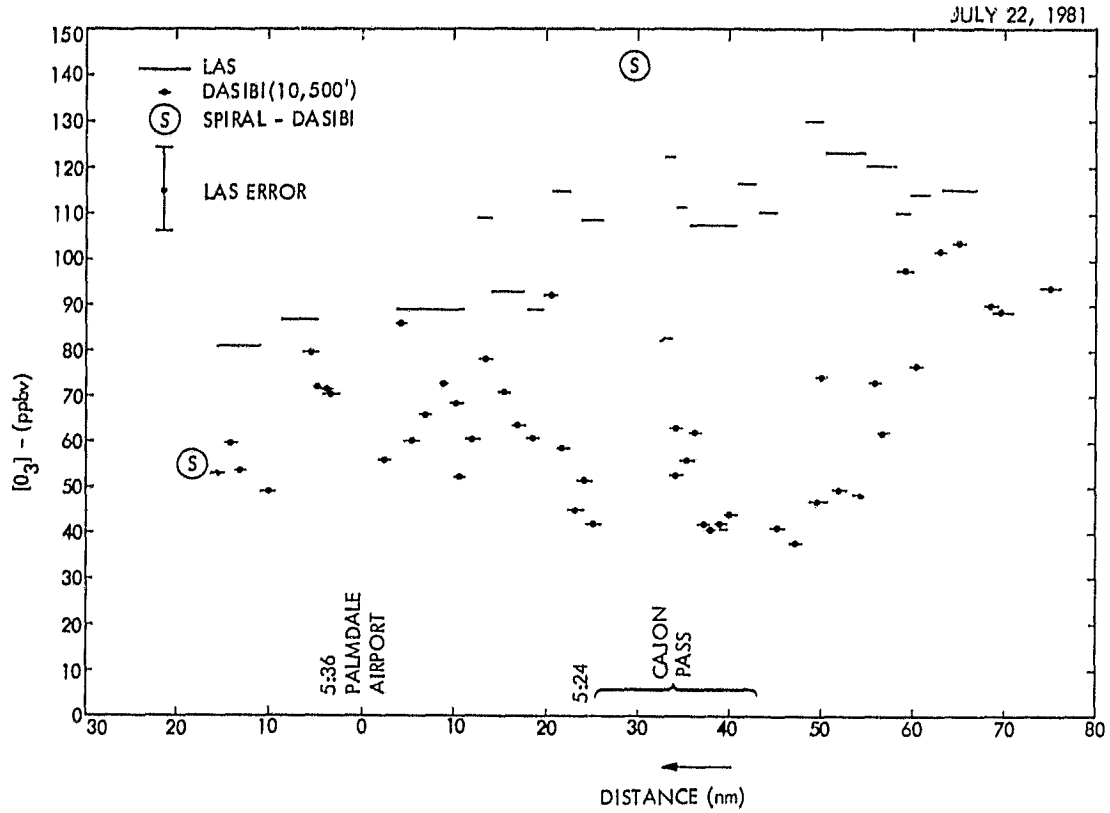

Figure 2-20. Ozone Measured in the Desert North of the San Gabriel and San Bernardino Mountains During the Second Flight of July 22, 1981

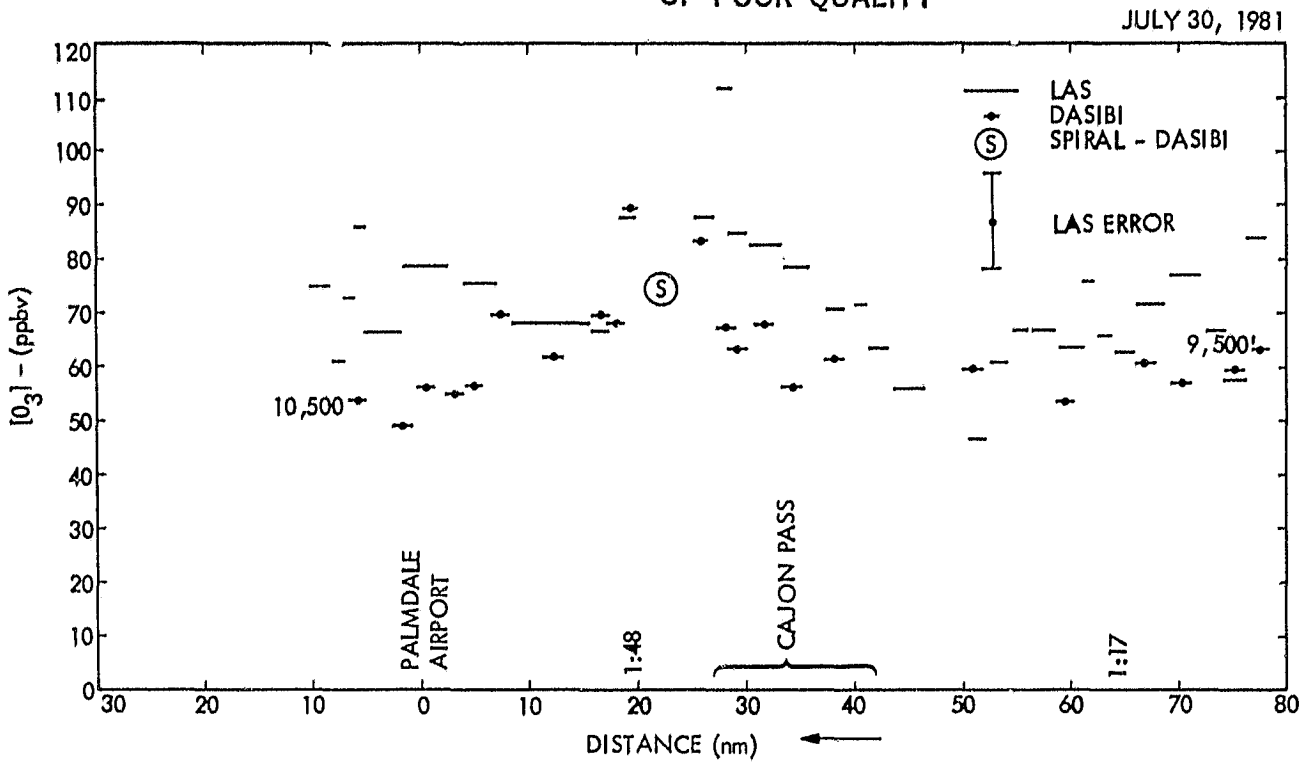

Figure 2-21. Ozone Measured in the Desert North of the San Gabriel and San Bernardino Mountains During the First Flight of July 30, 1981

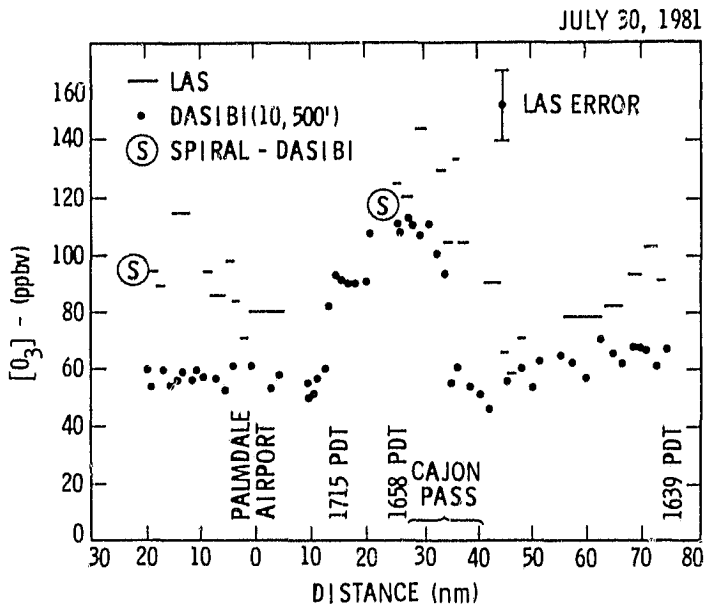

Figure 2-22. Ozone Measured in the Desert North of the San Gabriel and San Bernardino Mountains During the Second Flight of July 30, 1981

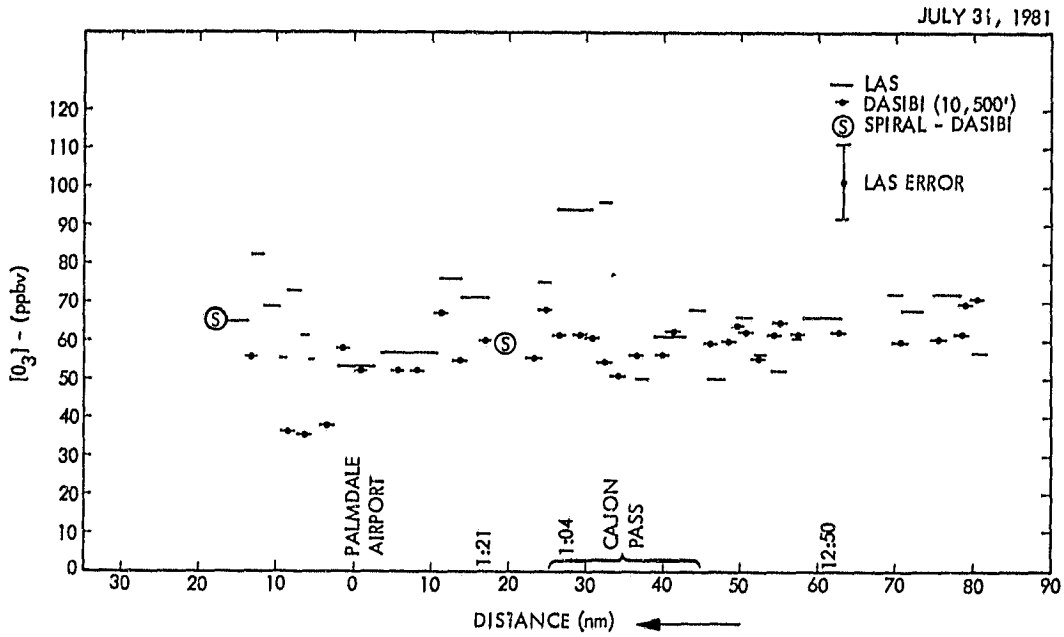

Figure 2-23. Ozone Measured in the Desert North of the San Gabriel and San Bernardino Mountains During the First Flight of July 31, 1981

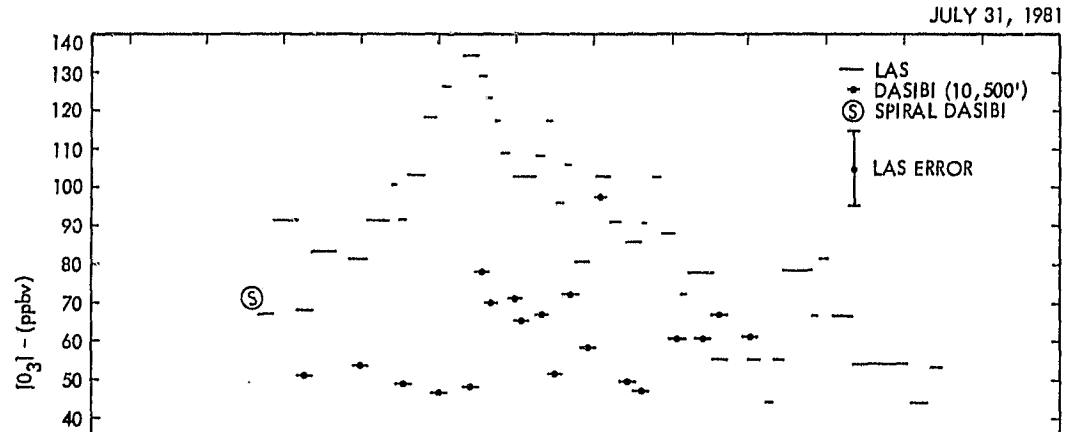

Figure 2-24. Ozone Measured in the Desert North of the San Gabriel and San Bernardino Mountains During the Second Flight of July 31, 1981

2.6 OZONE TRANSPORT FROM SAN GABRIEL VALLEY TO THE MOJAVE DESERT

Three additional figures were prepared that take the ozone data for the afternoons of July 22, 30, and 31 (Figures 2-14 and 2-20, 2-16 and 2-22, and 2-18 and 2-24, respectively) and place the measured values on a map of the region. Figure 2-25 for July 22 shows an ozone bulge in the San Gabriel Valley south of San Bernardino and north of Big Bear Lake in the desert. Figure 2-26 for July 30 shows an ozone bulge on both sides of the Cajon Pass. Figure 2-27 for July 31 shows a bulge in the San Gabriel Valley near Azusa and in the desert directly north of Azusa. These three figures indicate that ozone might be transported across the mountains or through the Cajon Pass.

The radiosonde winds data taken by Meteorology Research, Inc. (MRI) and the vertical profiles of ozone taken by JPL and MRI provide the extra data required to show that ozone transport was indeed from the San Gabriel Valley to the Mojave Desert. On July 22 near Fontana, the wind at 4 p.m. had a layer from 996 m (3,170 ft) to above 1,880 m (6,160 ft) that was blowing from the southwest. This was correlated with a layer of higher concentration ozone from 5,500 to 6,200 ft (see Figure 2-9). The mountains are about 7,000 ft high at this point. Thus, this ozone layer was most likely transported over the mountains by the southwest wind.

On July 30 at Redlands, the winds were blowing from the southwest above 1,170 m (3,830 ft) at 4 p.m. and from the south above 1,350 m (4,440 ft) at 6 p.m. The ozone vertical profiles for July 30 (Figure 2-11) do not indicate the presence of a layer of ozone above the mixing layer below about 3,500 ft, except east of the Banning Pass. The combination of winds from the south and the localization of high ozone concentrations near Cajon Pass in the Mojave Desert indicate that ozone was being blown through the Cajon Pass.

No comparable winds data were available for July 31. However, it seems consistent with the data of July 22 and July 30 that ozone was being blown across the mountains north of Azusa.

2.7 LAS MEASUREMENT ACCURACY

There are several primary sources of error for the LAS:

- Variations in differential spectral reflectance of the ground cover[2-6]
- Pressure variation of the ozone absorption coefficients
- Imprecise knowledge of the air-to-ground distance
- Error in the measurement of the ozone vertical profile
- Mechanical, optical and electrical variations in the LAS

Each will be discussed here with an estimate of its contribution to the total error.

Differential spectral reflectance for the P(24) - P(26) pair of lines could change as much as 5%, but would average 1-2% for typical ground covers. It would be more pronounced in the urban regions, with houses, streets, vegetation and open terrain, than in the desert regions. Indeed, the data in the San Gabriel Valley were much noisier than the data in the desert. The air-to-ground distance was typically 7,700 ft. One hundred parts-per-billion ozone concentration over that length (round-trip) would produce a 25% differential absorption. Thus, differential spectral albedo could give up to a 20 ppb uncertainty in the ozone measurement for a 5% effect. In this report, it is assumed that in

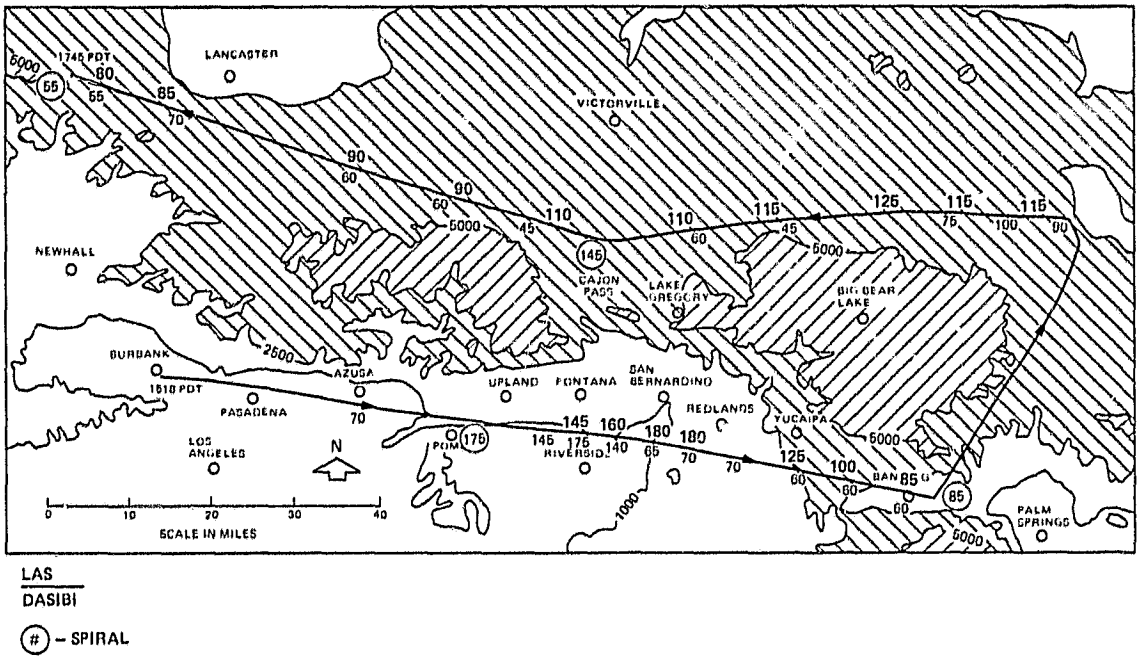

Figure 2-25. Measured Ozone Concentrations and Burdens for the Second Flight of July 22, 1981. The boldface numbers above the flight track are the column-content values measured by the LAS; the light numbers below the flight track are the values measured by the Dasibi Ozone Monitor at the flight altitude; the circled numbers are the column-content values determined using the Dasibi during a vertical spiral.

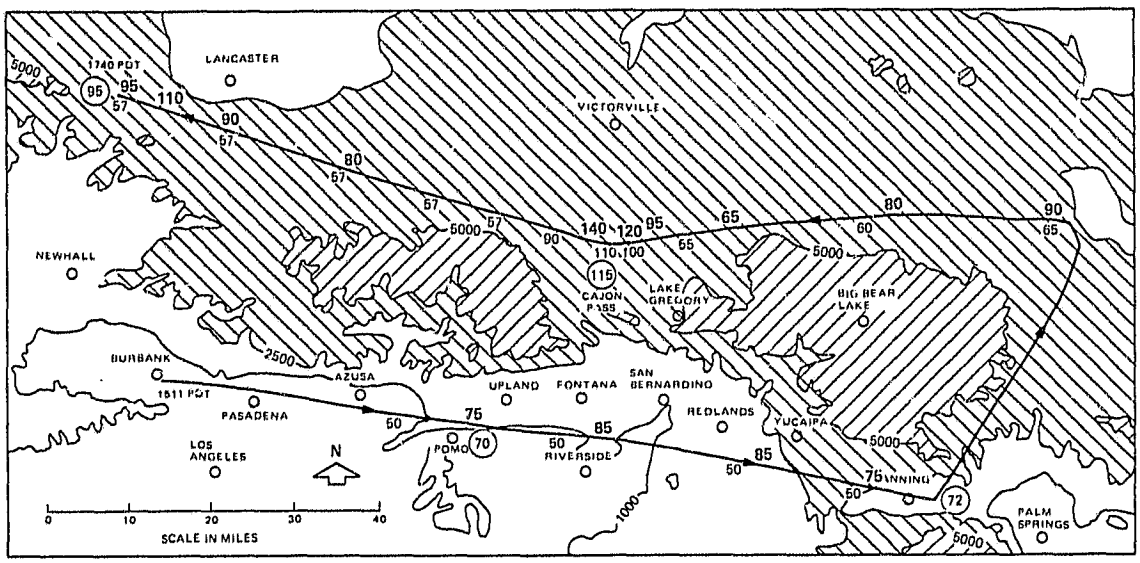

Figure 2-26. Ozone Values Measured During the Second Flight of July 30, 1981

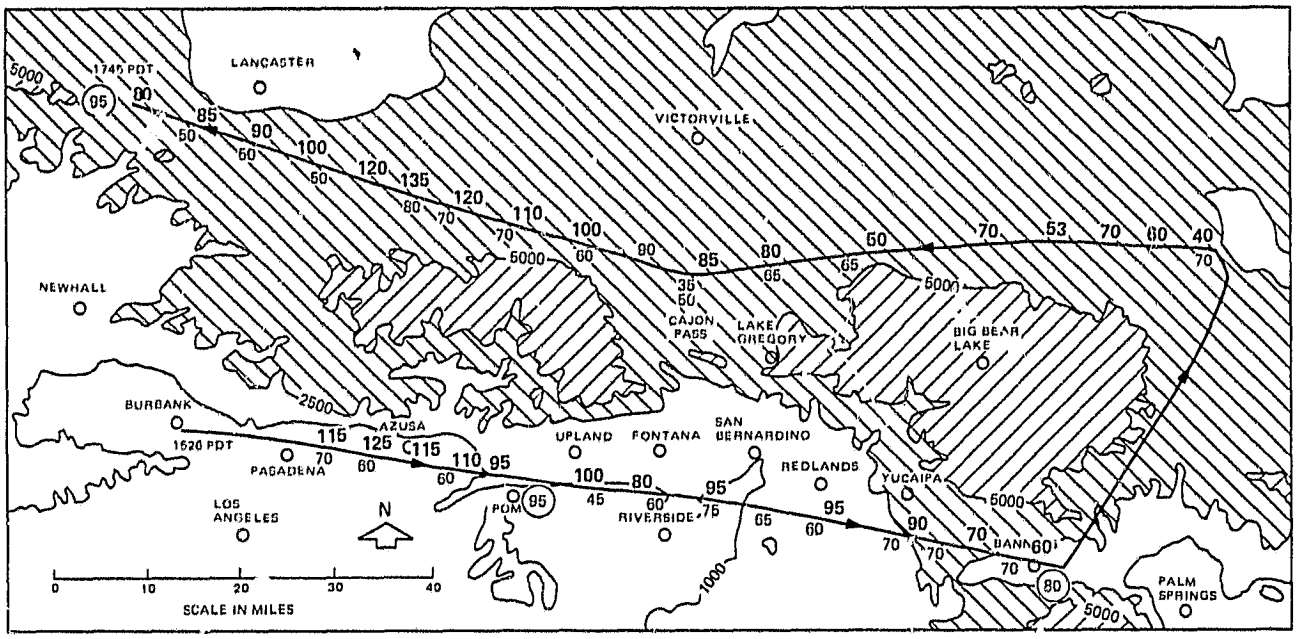

LAS
DASIBI

(#) – SPIRAL

Figure 2-27. Ozone Values Measured During the Second Flight of July 31, 1981

the San Gabriel Valley, this error is ±10 ppb, while in the deserts only ±5 ppb. The Valley is assumed to have the large error due to the greater variety of surface types.

Pressure variation of the ozone absorption coefficients can also affect the measurement accuracy. This is expected to account for a measurement uncertainty of ±4 ppb.

Imprecise knowledge of the air-to-ground distance affects the measurement accuracy because a concentration-pathlength is being measured. Typical height uncertainties were on the order of a 100 to 300 ft. For a height of 7,700 ft, 300 ft represents a 4% error or about ±4 ppb.

Error in the spiral measurement of the ozone at various points along the flight track can be a significant cause of measurement error. Sometimes, notably near the Cable Airport or Fontana, it seemed that industrial effluents were scavenging ozone. The 30-second averaging time for each Dasibi measurement limited the vertical resolution to 300 ft to 5,000 ft at the climb rates used during the measurements. When the mixing layer was shallow, few measurements were made in it. The Dasibi is somewhat sensitive to acceleration by the aircraft, such as when it is turning, and that could add 5-10 ppb to the uncertainty. Considering all of these errors, the average determined from the vertical profile is probably accurate to only about ±10 ppb in the Los Angeles Basin and ±5 ppb in the deserts.

Mechanical, optical and electrical variations in the LAS play a role, too. They were especially noticeable during the first leg of the flight - from Burbank to Cable Airport, as the lasers warmed up. This could have been alleviated by flying for 15-20 minutes at the desired altitude before starting the first data gathering leg of the flight. Also, there were drifts in the internal calibration measurement of a few percent (one percent here corresponds to 4 ppb) over 20 to 40 nm, which were assumed to vary linearly between calibrations, but may not have. Sometimes after a spiral, it was observed that the Ψ_0 had shifted by an amount equal to 20-ppb ozone, and the data were adjusted accordingly. These uncertainties were on the order of ±5 ppb for the data reported.

In summary, the errors are approximately:

Table 2-2. Sources and Magnitudes of LAS Errors

	Inside LA Basin (ppb)	In Deserts (ppb)
Differential spectral reflectance	±10	± 5
Pressure variation of absorption coefficients	4	4
Air-to-ground distance	4	4
Measurement of ozone vertical profile	10	5
Mechanical, optical and electrical	5	5
Total (RMS)	±16	±10

2.8 REFERENCES

2-1 R. T. Menzies and M. S. Shumate, "Tropospheric Ozone Distributions - Measured with an Airborne Laser Absorption Spectrometer," J. of Geophysical Research, 83, No. C8, p. 4039 (1978).

2-2 M. S. Shumate, R. T. Menzies, W. B. Grant and D. S. McDougal, "Laser Absorption Spectrometer: Remote Measurement of Tropospheric Ozone," Appl. Opt., 20, No. 4, p. 545 (1981).

2-3 W. B. Grant and M. S. Shumate, "Remote Measurments of Ozone Burden in the LA Basin on September 20 and 24, 1979, using the Airborne Laser Absorption Spectrometer," Final report 5030-442 to NASA Office of Technology Utilization (1980).

2-4 M. S. Shumate, "Participation of the JPL Laser Absorption Spectrometer in the 1980 PEPE/NEROS Program in Columbus Ohio," Final Report #715-84 to NASA and EPA (1980).

2-5 M. S. Shumate, W. B. Grant, and R. T. Menzies, "Remote Measurement of Trace Gases with the JPL Laser Absorption Spectrometer," in Optical and Laser Remote Sensing, D. K. Killinger and A. Mooradian, eds., Springer Verlag, Berlin, p. 31 (1983).

2-6 M. S. Shumate, S. Lundqvist, U. Persson, and S. T. Eng, "Differential Reflectance of Natural and Man-made Materials at CO_2 Laser Wavelengths," Appl. Opt., 21, 2386 (1982).

2-7 J. Boscher, G. Schafer, and W. Wiesemann, "Gasfernanalyse mit CO_2-Laser," Batttelle Institut e.V., D-6000 Frankfurt am Main, West Germany (1979).

2-8 R. T. Menzies, "Ozone Spectroscopy with a CO_2 Waveguide Laser," Appl. Opt., 15, No. 11, p. 2597 (1976).

2-9 W. Schnell and G. Fischer, Observatoire Cantonal, Neuchatel, Switzerland, Private communication (1975).

3.0 FREQUENCY-MODULATED CO_2-LASER REMOTE MEASUREMENT OF OZONE

3.1 INTRODUCTION

There is an increasing need to remotely sense atmospheric trace gases. In some cases, it is difficult to physically enter the geographical region of interest.[3-1] In other cases, it is difficult otherwise to sample the gas without destroying its integrity,[3-1] or to monitor its concentration in real time. Finally, there are cases where time and money can be saved by remote sensing.

One active remote-sensing technique being developed is the differential absorption lidar (DIAL) technique.[3-2] In this approach, usually two laser wavelengths are used: one wavelength is chosen at which the gas of interest absorbs strongly; the other is chosen at which the gas absorbs weakly, and acts as a reference line. A ratio of the return signals at the two wavelengths is used to determine the gas concentration using Beer's law for an absorbing medium.

In the majority of DIAL systems, direct detection of the return signal is employed. The detector registers a signal which is proportional to the backscattered laser radiation, as well as the background radiation within the bandpass of the optical filter and/or detector. Some of these systems have used CO_2 lasers in a pulsed mode of operation with atmospheric backscatter to measure H_2O[3-3] and O_3,[3-4] or with topographic targets to measure C_2H_4,[3-5] N_2H_4[3-6] and atmospheric temperature.[3-7] The idea of using CO_2 lasers with topographic targets to measure atmospheric trace gases was suggested in 1967 by Jacobs and Snowman.[3-8]

Lidar systems have also been constructed that use heterodyne detection of the backscattered laser radiation. In this approach, one laser acts as a local oscillator to activate the detector, and a second laser can be used to transmit laser power to a target. The two lasers are adjusted to have a frequency separation of usually a few megaHertz. The heterodyne-detection approach allows RF-detection electronics to be used, and eliminates background radiation outside of the bandwidth of the electronics.[3-9] This allows much weaker signals to be detected than with direct detection. This approach was first used with cw CO_2 lasers to measure O_3, using topographic targets.[3-10]

The coherent-detection technique can also be used with one laser acting as both the local oscillator and the transmitting source, in a modified homodyne technique. This is the basis of operation of the JPL Laser Absorption Spectrometer (LAS),[3-11] which has a pair of CO_2 waveguide lasers, and is flown and aimed slightly ahead of nadir so that a 3-MHz Doppler frequency shift is obtained. This approach has been used to measure O_3,[3-11,3-12] SF_6[3-13] and quartz on the Earth's surface.[3-13]

This approach can be taken a step further by frequency-modulating the laser wavelength and allowing the round-trip time-of-flight to produce the desired frequency shift. It is sometimes referred to as the FM-CW lidar technique. This has been studied in detail for one CO_2 lidar aimed at solid targets.[3-14] It has also been proposed for application to the remote measurement of gases using the DIAL technique.[3-15] The advantage of this approach over that of using pulsed lasers is that lower average-power lasers can be used with coherent detection than with direct detection, because coherent detection can be 2-3 orders of magnitude more sensitive,[3-9] and because the data system can be much simpler for a cw rather than pulsed system.

This paper describes the adaptation of the LAS[3-11] for the FM-CW DIAL lidar technique by modulating the cavity length, hence the laser wavelength, and its use in a demonstration measurement of O_3 in the ambient air.

3.2 EXPERIMENTAL APPARATUS

The LAS is described in Reference 3-11 and in Section 2 of this report. The only modification to the LAS was the application of a sawtooth-voltage drive to the piezoelectric bimorphs[3-16] on which the gratings are mounted.

The P(14) and P(22) lines in the 9.5 μm spectral region were used for the measurements of ozone. The absorption coefficients for O_3 for these lines are 13.0 ±0.3 and 1.9 ±0.1 $atm^{-1}cm^{-1}$ respectively.[3-11]

3.3 MEASUREMENT RESULTS AND DISCUSSION

O_3 was measured from a site overlooking an area in the arroyo slightly below the elevation of the laboratory. Several targets visible from the laboratory were used to provide the backscattered signal. In order to estimate the concentration of O_3 that the lidar system should be measuring, a Dasibi ozone monitor stationed near the lidar was used to measure the ambient ozone concentrations.

Measurement results for O_3 using trees as targets at 0.9 and 1.5 km are shown in Figures 3-1 and 3-2. Each data point represents a four-minute average. During the four minutes, the ratio of the return signals for the P(14) and P(22) lines varied by about ± 0.05, which is equivalent to ±20 ppb. The variation of the LAS-determined O_3 concentration from the Dasibi-determined O_3 concentration was ±10 ppb using the tree at 0.9 km, and ±20 ppb using the tree at 1.5 km. For the two more distant targets, the variations were about ± 30-40 ppb. The lines on the graphs are a best fit to the data using Beer's law for an absorbing medium.

Of the several sources of measurement error, one is due to electro-opto-mechanical instrumental drift. For example, the laser cavity length changes as the laser temperature changes, and the laser amplitude-vs-voltage response changes somewhat with offset voltage applied to the bimorph. To reduce drift, the modulation amplitude was maintained at 2.7% of laser power. However, since the modulation envelope changes with temperature of the laser, the frequency modulation changes as well, and some of the return signal is filtered out. As shown in Reference 3-14, the signal is not a delta function, but has a long tail to low frequencies. The transmitter/receiver overlap, which is sensitive to changes changes in laser-pointing direction (possibly caused by changes is the laser mode pattern) and detector position, can affect the measurement, and may be responsible for the day-to-day changes in system response to a given concentration of O_3.

Spectral interference from other gases can be a problem, but not a major one for the P(14)/P(22) line pair. A change in the CO_2 concentration of 100 ppm is equivalent to 2 ppb O_3;[3-17] an increase of ethylene by 150 ppb is measured at a 10 ppb decrease in O_3;[3-18] and H_2O has a very small effect on the O_3 measurement.[3-19]

Differential spectral reflectance (DSR), or the change in reflectance of a target with wavelength, has to be considered with any laser system that uses topographic

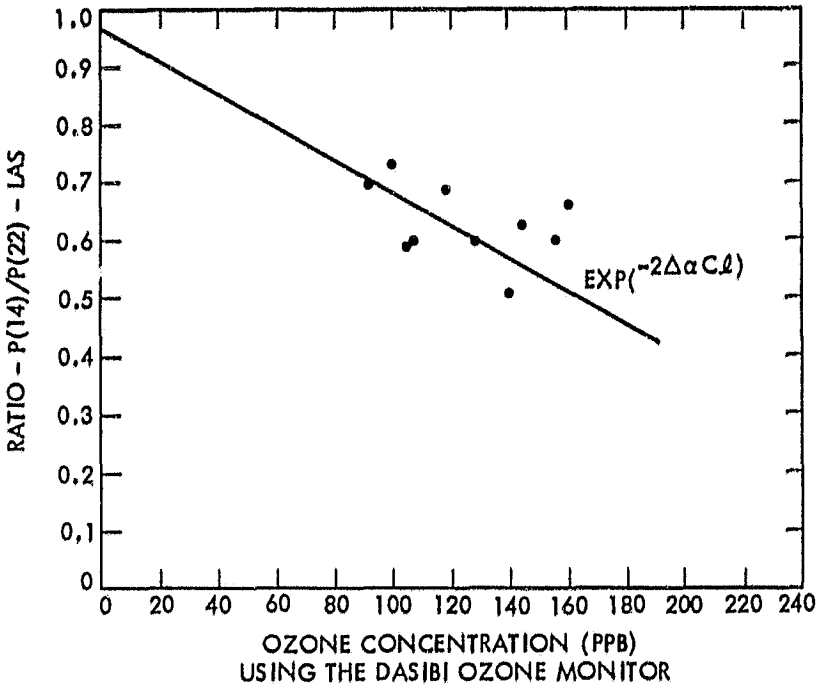

Figure 3-1. Comparison of Ozone Concentrations Measured Using the Dasibi Ozone Monitor and the LAS in the FM-CW Mode for a Target Distance of 1.5 km

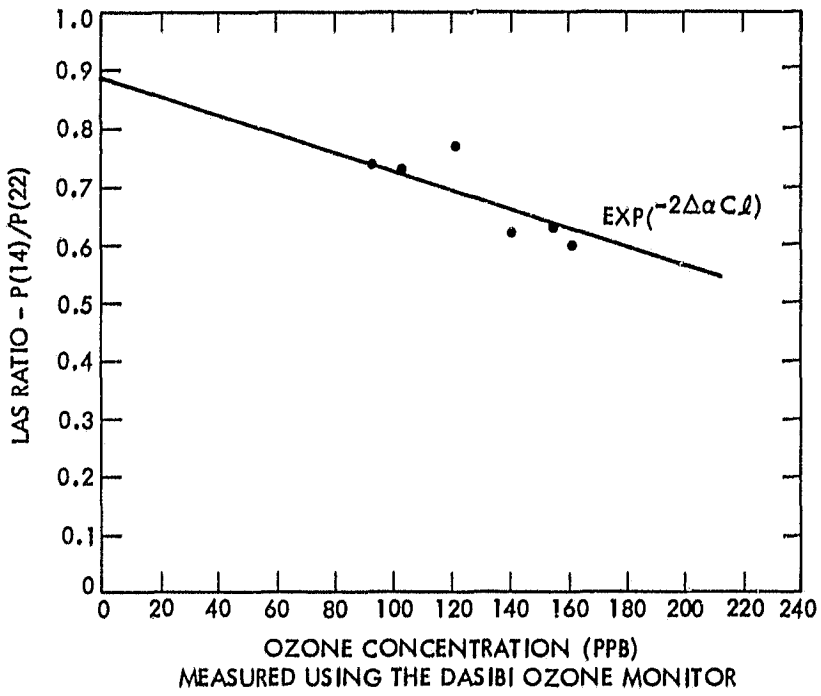

Figure 3-2. Comparison of Ozone Concentrations Measured Using the Dasibi Ozone Monitor and the LAS for a Target Distance of 0.9 km

targets to provide the backscattered signal.[3-12,3-20 - 3-22] The P(14/P(22) CO_2-laser pair is particularly susceptable to this effect because of its large wavelength separation (7 cm^{-1}), and the existence of rapid variations in the reflectance spectrum with wavelength of some materials in this spectral region. However, the repeated use of fixed targets allows the DSR effect to be calibrated out for each target. If a number of targets have to be used in rapid succession, chosing vegetation targets where possible would reduce the DSR effect.[3-21]

The effect of atmospheric turbulence on the speckle pattern is perhaps the most serious problem.[3-23 - 3-25] Since the speckle-lobe diameter is expected to be about the diameter of the transmitter or receiver aperture (5 cm) for a flat target, if a speckle lobe wanders in and out of the receiver field-of-view, it can cause large intensity fluctuations. Flat surfaces were found to give much larger intensity fluctuations than were irregular surfaces, in agreement with Reference 3-21. The irregular surface acts as a multiple source of reflection, giving a signal with much less coherence.

One other problem that occurs more with small targets is the lack of complete convergence on the target of the two transmitted beams from the LAS. This arises from the particluar design of the LAS, and is not an inherent problem of the technique.

3.4 FUTURE IMPLICATIONS

While the LAS is a bulky system, future systems could be made that are much smaller and more convenient to use in the field, by using closed-cycle CO_2 waveguide lasers and miniaturized electronics. The gases may be either uniformly mixed in the ambient atmosphere or in plumes coming from point sources.[3-26] Based on the measurement accuracy demonstrated with this system for O_3 ($\pm$ 2.2% or $\pm$ 10 ppb-km), the measurement accuracy for other gases can be calculated. Results are given in Table 3-1.

Table 3-1

Parameters for Molecular Species Measurable Using a CO_2 Laser System

Molecular Species	Wavelengths On (μm)	Wavelengths Off (μm)	Diff. Absorption Coefficient ($atm^{-1}cm^{-1}$)	Measurement Sensitivity (ppb-km)
C_2H_4	10.532	10.551[3-10]	24.6[3-17]	5
C_3H_5OH	9.676	9.658	19.6[3-18]	6
C_2HCl_3	10.608	10.588	4.9[3-17]	23
H_2O	10.247	10.260[3-3]	$7.7.10^{-4}$[3-27]	150 (ppm-km)
NH_3	9.217	9.227	55.8[3-28]	2
N_2H_4	10.718	10.696[3-6]	3.5[3-17]	32
O_3	9.503	9.569[3-11]	11.3[3-29]	10

In addition to measuring gases, the system could be used for measuring the chemical position of opaque aerosol clouds using the DIfferential SCattering (DISC) technique.[3-30] In the DISC technique, the backscatter of laser radiation at several wavelengths is used to distinguish aerosols of different composition. It could also be used to identify rock types.[3-13,3-20 - 3-22]

3.6 REFERENCES

3-1 W. A. McClenny and G. M. Russwurm, Atmos. Environ., 12, 1443 (1978).

3-2 E. D. Hinkley, Editor, Laser Monitoring of the Atmosphere, Springer Verlag, New York (1976).

3-3 E. R. Murray, J. R. van der Laan, and J. G. Hawley, Appl. Opt., 15, 3140 (1976).

3-4 K. Asai, T. Itabe, and T. Igarashi, Appl. Phys. Lett., 35, 60 (1979).

3-5 E. R. Murray and J. E. van der Laan, Appl. Opt., 17, 814 (1978).

3-6 N. Menyuk, D. K. Killinger, and W. E. DeFeo, Appl. Opt., 21, 2275 (1982).

3-7 E. R. Murray, D. D. Powell, and J. E. van der Laan, Appl. Opt., 19, 1794 (1980).

3-8 G. B. Jacobs and L. R. Snowman, IEEE JQE, QE-3, 603 (1967).

3-9 R. T. Menzies in Laser Monitoring of the Atmosphere, Edit. by E. D. Hinkley, Springer Verlag, New York, pp 297-353 (1976).

3-10 R. T. Menzies and M. S. Shumate, Appl. Opt., 15, 2080 (1976).

3-11 M. S. Shumate, R. T. Menzies, W. B. Grant, and D. S. McDougal, Appl. Opt., 20, 545 (1981).

3-12 W. B. Grant, "Measurement of Ozone Transport from the Los Angeles Basin Using the Airborne Laser Absorption Spectrometer and a Dasibi Ozone Monitor," Final Report #5030-512 by the Jet Propulsion Laboratory, California Institute of Technology, to the California Air Resources Board (1981).

3-13 W. Wiesemann, R. Beck, W. Englisch, and K. Gurs, Appl. Phys., 15, 257 (1978).

3-14 G. Bolander, K. Gullberg, I. Renhorn, O. Steinvall, and A. Widen, "Studies of Target Signatures with a Coherent Laser Radar," FOA Report C 30220-E1, Forsvarets Forskningsanstalt, Huvudavdelning 3, Box 1165, 581 11 Linkoping, Sweden (May 1981).

3-15 T. Kobayasi, M. Hamza, H. Ishihara, and H. Inaba, "High Sensitive and Compact Laser Radar Using FM Optical Heterodyne Technique." Paper presented at the Tenth International Laser Radar Conference, Silver Spring, MD (1980). Sponsored by the American Meteorological Society, Boston, MA.

3-16 Vernitron Piezoelectric Div., Vernitron Corp., 232 Forbes Rd., Bedford, OH 44146.

3-17 R. R. Patty, G. M. Russwurm, W. A. McClenny, and D. R. Morgan, Appl. Opt., 13, 2850 (1974) (plus private communication.)

3-18 G. L. Loper, A. R. Calloway, M. A. Stamps, and J. A. Gelbwachs, Appl. Opt., 19, 2726 (1980).

3-19 R. J. Nordstrom, M. E. Thomas, J. F. Donavan, and K. Gass, "Atmospheric Water Vapor Absorption at 12 CO_2 Laser Frequencies," Final Report 711934-1 by Ohio State University, Electro-Science Laboratory, to JPL (1979).

3-20 J. Boscher and F. Lehman, "Experimentelle Untersuchungen der physikalischen Grundlagen zur fernmessung von Boden- und Vegetationsfeuchte durch aktive Intrarot-Reflexionsspektroskopie mit Hilfe der CO_2-Lasertechnik." Report 01 QS 039-AK/WF/RT 1078-3.2 by Battelle Institut e.V., Frankfurt, W. Germany (1980).

3-21 M. S. Shumate, S. Lundqvist, U. Persson, and S. T. Eng, Appl. Opt., 21, 2386 (1982).

3-22 W. B. Grant, Appl. Opt., 21, 2390 (1982).

3-23 N. Menyuk and D. K. Killinger, Opt. Lett. 6, 301 (1981).

3-24 J. F. Holmes (Oregon Graduate Center), "The Effects of Target Induced Speckle, Atmospheric Turbulence, and Beam Pointing Jitter on the Errors in Remote Sensing Measurements," presented at the "Workshop on Optical and Laser Remote Sensing", Monterey, CA (sponsored by the U. S. Army Research Office, Research Triangle Park, NC (9-11 February 1982).

3-25 P. H. Flamant, R. T. Menzies and M. J. Kavaya, (JPL), "Statistical Properties of CO_2 Lidar Returns from Topographic Targets", presented at the Eleventh International Laser Radar Conference, Madison, Wisconsin (sponsored by the American Meteorological Society, Boston, MA). (June, 1982).

3-26 W. B. Grant and E. D. Hinkley, "Laser System for Natural Gas Detection - Phase I - Laboratory Feasibility Studies," Annual Report #5030-525 by JPL for the Gas Research Institute (July 1982).

3-27 M. S. Shumate, R. T. Menzies, J. S. Margolis, and L. G. Rosengren, Appl. Opt., 15, 2480 (1976).

3-28 R. J. Brewer and C. W. Bruce, Appl. Opt., 17, 3746 (1978).

3-29 R. T. Menzies, Appl. Opt., 15, 2597 (1976).

3-30 H. T. Mudd, Jr., C. H. Kruger, and E. R. Murray, Appl. Opt., 21, 1146 (1982).

4.0 DEMONSTRATION OF A MICROWAVE REMOTE SENSOR SYSTEM FOR THE MEASUREMENT OF ATMOSPHERIC TEMPERATURE PROFILES AND CLOUD LIQUID WATER CONTENT

4.1 BACKGROUND AND INTRODUCTION

Passive microwave techniques for remote sensing of atmsopheric properties has its origins in the 1960's (see Reference 4-1 for an extensive review). Ground-based systems demonstrated the validity of theoretical predictions, and showed that passive measurements at specific frequencies should enable determinations to be made of 1) line-of-sight content of water vapor,[4-2 - 4-4] 2) line-of-sight content of (cloud) liquid water,[4-3] and 3) temperature versus altitude.[4-5,4-6] These early demonstrations were limited by poor radiometer sensitivity, incomplete frequency sampling, and unsophisticated retrieval algorithms. The technology was "picked-up" by the "earth satellite community," and great strides forward were made in each of the three areas that had been limiting in the earlier ground-based usage.[4-7] JPL built the Nimbus 5 "NEMS" (Nimbus E Microwave Spectrometer) and Nimbus 6 "SCAMS" (Scanning Microwave Spectrometer). These were satellite-based 5-frequency radiometers that have successfully demonstrated "down-looking" capabilities.[4-8]

After successful launch and operation of the NEMS and SCAMS satellite instruments, a unique combination of hardware and remote sensing "know how" resided at JPL. This was seen as an oportunity for returning to the unfinished task of ground-based sensing without the earlier limitations. The NOAA Data Buoy Office, in cooperation with the NASA/OSSA Technology Transfer Division, funded JPL to demonstrate this new capability for a maritime setting, using a modified SCAMS instrument. A successful concept demonstration was performed in 1978 on the weathership Quadra, stationed in the Gulf of Alaska.[4-9] Temperature profiles, water vapor, and liquid water were measured. Measurements agreed with comparison radiosondes. We are now constructing an automated, compact 7-frequency radiometer system for installation (in 1983) in a "deep ocean, moored" buoy.

In parallel with the buoy project, JPL has been constructing a land-based system which can be used for air pollution studies. A significant stage in the evolution of this project occured with the 1980 deployment of a microwave system for participation in the EPA- directed PEPE/NEROS Experiment (Persistent Elevated Pollution Episodes/Northeast Regional Oxidant Study).[4-10] The JPL system was called MARS (Mobile Microwave Atmospheric Remote Sensing System). MARS measured the same atmospheric parameters as those measured by the buoy system. A borrowed water vapor radiometer and a borrowed "low-altitude temperature profiling radiometer" were used.

NASA/OSSA Technology Transfer funds have been used to complete the MARS. The borrowed radiometers have been replaced with dedicated radiometers "tailored" to their jobs. Numerous small improvements have been made. The first observations with the new MARS were conducted in 1982. NASA paid for initial calibrations (against radiosondes) in May, 1982, thus completing NASA's role in transfering the MARS technology.

California Air Resources Board funds were then used to provide MARS meteorology support to the Caltech field study of "acid fog," in June, 1982. The temperature "channels" were not operating properly at that time, and only cloud liquid water

and water vapor data were obtained (this data set is judged to be adequate for supporting the Caltech study). The new MARS has been used recently in its "fullup" capability for the primary purpose of monitoring overhead temperature profiles. Comparisons with radiosondes have been made, but no smog-related inversion structures have been encountered to provide the sought-for "evaluation of usefulness" for smog-forecasting applications. Computer simulations have been conducted, though, and these results indicate that good performance during strong inversions conditions can be expected.

4.2 DESCRIPTION OF WHAT IS MEASURED

The new MARS system measures "sky brightness temperature" at five microwave frequencies - 22.2, 31.4, 54.0, 55.3, and 57.5 GHz (gigahertz) - for a selection of elevation angles (from 5 degrees to zenith). Supporting non-microwave measurements are made of OAT (outside air temperature), RH (relative humidity), BP (barometric pressure), and IR sky brightness temperature (8-14 m). In all, there are 20 "observables" generated by MARS for the retrieval of meteorological properties.

The meteorological properties that are derived from the 20 observables can be summarized:

(1) Altitude temperature profiles (ground level to 10,000 ft)
(2) Overhead water vapor (precipitable water vapor)
(3) Overhead cloud liquid water (zenith integrated total)
(4) Altitude of the cloud base (when clouds are present)
(5) Liquid water concentration (average for the cloud layer)

Items 2 and 3 have been derived by our group with MARS type hardware for many years, and we have a great deal of confidence in the quality of these products. Item 1, the temperature profiles, has been worked with for 4 years, and our capabilities in this area are growing rapidly. Items 4 and 5 were demonstrated during the "aviation icing monitoring" field demonstration, conducted for the Air Force in March 1983 (described in a report, Reference 4-11, which is available upon request).

The water vapor and liquid water parameters are obatained from the 22.2- and 31.4-GHz observables. The temperature profiles are generated prinicipally from the 54.0, 55.3, and 57.5 GHz observables. Corrections related to water vapor and liquid water are applied to these observables. Cloud base altitude (ceiling) is deduced from the IR brightness temperature measurement, in combination with the altitude temperature profile derived from the microwave observables. Liquid water concentration within a stratus cloud layer is derived from a combination of the zenith integrated liquid-water content, the cloud base altitude, and the cloud top altitude (assumed equal to the temperature inversion base altitude).

The underlying theory that enables MARS observables to be converted to meteorology properties have been described elsewhere.[4-12] Briefly, the 22.2-GHz observable is most sensitive to thermal emission by water vapor molecules, the 31.4-GHz observable is most sensitive to thermal emission by liquid water (cloud) droplets, and the 54.0, 55.3, and 57.5-GHz observables are responsive to thermal emission of oxygen molecules at ranges of approximately 7,000 ft, 3,400 ft, and 1,400 ft. Angle scanning of the three "oxygen" radiometers ena-

bles a suite of altitudes (below their applicable range) to be probed. A variety of "retrieval" techniques are available for conversion of observed brightness temperature to air temperature versus altitude. A statistical retrieval algorithm is used for real-time reduction.

4.3 DESCRIPTION OF INSTRUMENT

The MARS system is housed in a step van. The van has built-in generators, permitting operation in remote locations. Set-up time is about 30 minutes. All subsystems are controlled by an HP 9825 computer, which also performs such functions as: data recording, real-time reduction, and video display of results. Video displays of "altitude temperature profiles" are presented in the MARS van, and can be transmitted via phone line to any standard terminal (video or printing). These profiles are produced at 2-minute intervals.

The microwave radiometers have 1-second sensitivities of 0.5°C (54.0 and 55.3 GHz) 0.3°C (22.2 and 31.4 GHz), and 0.10°C (57.5 GHz). All antenna beamwidths are 7.5 degrees. Calibration accuracy is approximately 0.5°C, which is achieved by a unique technique of "inter-channel calibration."

4.4 MEASUREMENT RESULTS

4.4.1 Cloud Liquid Water Content

During June, 1982, the MARS system was deployed at Eaton Canyon (five miles northeast of downtown Pasadena) for coordinated observations with Caltech researchers studying acid fog. MARS measured liquid water content of overhead stratus clouds. Visual estimates of cloud base altitude were combined with radiosonde measurements of cloud top altitude (at two locations in the LA Basin) to derive cloud physical thickness. Liquid water content was divided by physical thickness to arrive at "liquid water concentration," LWC (g/m3). LWC should be correlated with fog acidity, which was being measured by the Caltech team. The MARS data have been described in a report that is included as Appendix A of this report.

4.4.2 Temperature Profiles

Our goal for temperature profiling was to conduct MARS observations during a smog alert and demonstrate the inversion layer monitoring capability using MARS data. In preparation for this we spent four days at the Southern California Edison Co. radiosonde launch site in Ontario, CA conducting MARS/radiosonde calibration comparisons (May 18-21, 1982).

In September 1982, we began observations at JPL for the purpose of monitoring temperature profiles through smog alerts. Good data were obtained during the Stage I ozone alerts on September 2 and 3. There was only one problem with this data: while downtown Pasadena was experiencing ozone laden air under low inversion layer conditions, JPL was experiencing very clean air at an altitude that was just above the inversion layer. Indeed, the MARS data showed adiabatic lapse rates after the burn-off of early morning ground-based inversions. This convinced us that JPL's altitude of 1,280 ft (where MARS was located) was too high above the nearby basin area to allow monitoring of the smog related inversions that we were after.

In order to maximize the probability for encountering strong overhead inversion layers, we decided to deploy MARS at a low elevation site close to the coast. The radiosonde launching site at Loyola Marymount University (LMU), near the Los Angeles International Airport, was chosen. A cooperative exchange of data was arranged with Erwin Kauper, who was under CARB contract for the radiosonde launchings. Our first MARS observations on September 23 were marred by radio interference problems. We modified the MARS radiometers to make them less vulnerable to interference from what we thought might be transmitters associated with the Los Angeles Airport, and return to the LMU site for observations on October 1. These data were good quality, but there was no inversion layer that day. We returned Oct. 14, and obtained good data, but again no inversion layer developed. We were on standby until scheduled LMU radiosonde launches ceased at the end of October. October was rainy, and offered few opportunities for encountering the low-level, strong inversion layers we were waiting for.

Since MARS observations on behalf of this CARB contract have been terminated, we are left with the question: how well does MARS monitor low-level, strong temperature contrast inversion layers (the kind associated with smog alerts)? In order to answer this question, without the benefit of observations that would answer it directly, we have conducted computer simulations. These simulations take into account the calibration and stochastic characteristics of MARS. The results of these simulations have been described in a way that answers the question: "how unique" can MARS temperature profile retrievals be? This write-up is included as Appendix B, "Uniqueness of Temperature Profile Retrievals." The answer produced by this analysis is that MARS should do very well for the inversion layers associated with smog alerts.

4.5 Buffalo Field Measurements with MARS

The MARS system was deployed last March (1983) in Buffalo, NY, for a field measurement program sponsored by the U.S. Air Force Geophysics Laboratory. The objective of this deployment was to evaluate the usefulness of MARS for monitoring "aviation icing hazard." The remote sensing demands of this task were more demanding than those of monitoring mixing depth for smog forecasting purposes. More comprehensive calibrations were conducted during the course of this project. Analysis of this data is two-thirds complete. A preliminary status report has been prepared, describing T(h), water vapor, and liquid water sensing performance. This report shows that MARS T(h) performance is close to theoretical predictions, which is RMS accuracy of 0.8°C from surface to 2,000 ft, 2°C at 5,000 ft, and 3.5°C at 10,000 ft.

Figure 4-1 is a sample "altitude temperature profile" produced by the MARS system during checkout observations at JPL in December 1982. The left margin is a vertical scale, labeled in thousands of feet, which shows that this particular display extends from surface to 7,300 ft. The horizontal scale is labeled in °C. The "0" pattern is "observed" brightness temperature, and the "#" pattern is retrieved air temperature. A statistical retrieval algorithm was used. A pattern of blanks indicates an adiabatic lapse rate line, shifted to intersect the surface temperature. Comparison of the retrieved air temperature profile with the adiabatic pattern shows that surface air must not be circulating vertically, since any surface air that would be lifted, and cooled adiabatically, would be cooler than ambient air, and possess negative buoyancy (and would thus fall back toward the surface). The lowest 300 ft

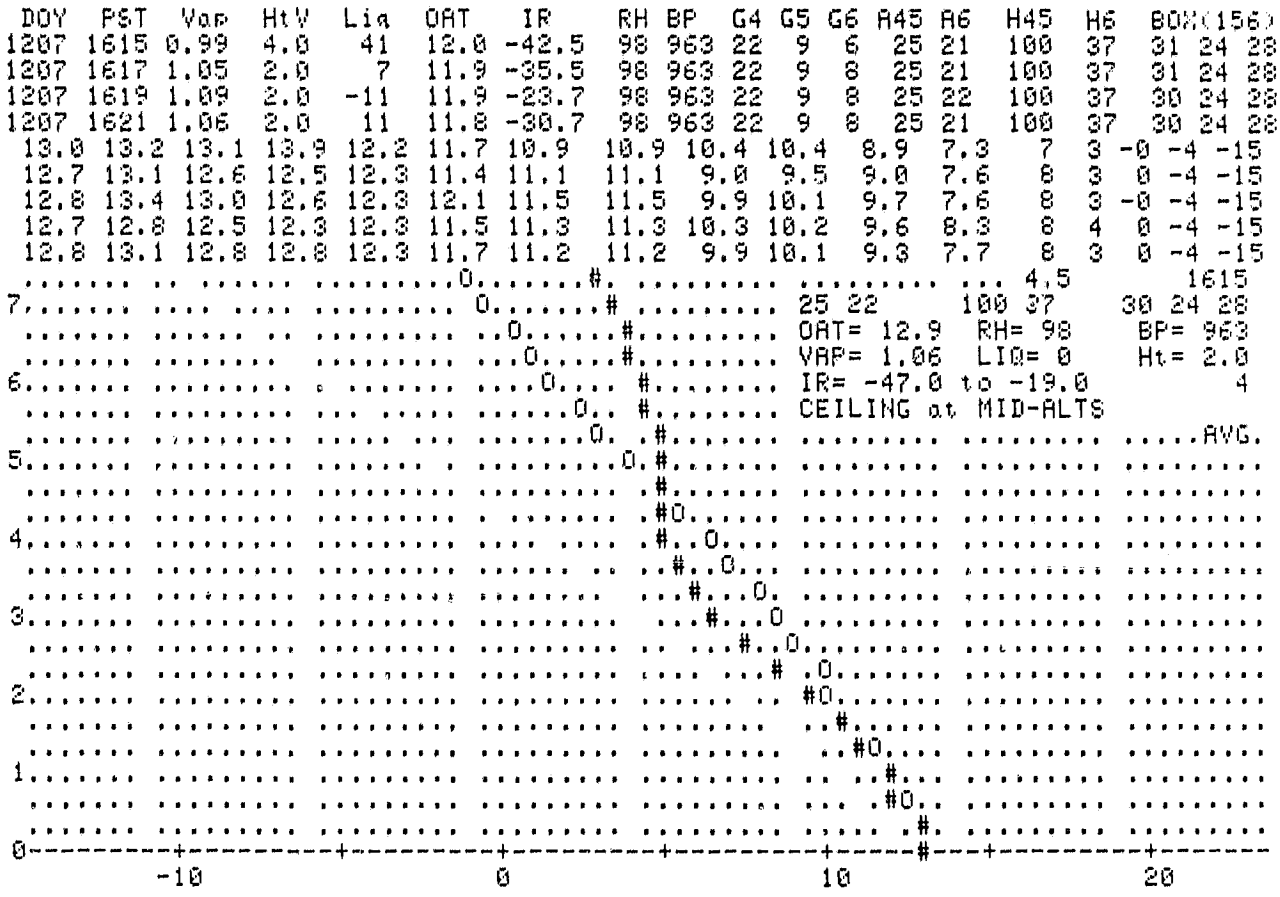

Figure 4-1. A Sample "Altitude-Temperature Profile" Produced by the MARS System. The vertical axis is in thousands of feet; the horizontal scale is in degrees C.

appear to be isothermal.

A "box" of information about this 8-minute observation period is presented in the upper-right corner. This box conveys the following information: data for the profile began December 7, 1982, at 1615 PST: instrument temperatures were 25°C, etc; outside air temperature was 12.9°C; relative humidity was 98%; barometric pressure was 963 millibars; precipitable water vapor (zenith-integrated water-vapor content) was 1.06 cm; zenith-integrated liquid-water content was 0 microns; assumed vapor-weighted altitude of the water vapor was 4,000 ft; IR zenith brightness temperatures ranged from -47.0°C to -19.0°C during the observing period; and, based on the maximum IR temperture, the cloud bases were at altitudes that could be described as "middle altitudes" (patchy thin clouds were present).

Altitude temperature profile panels like this one are presented in realtime in the MARS van, and can be transmitted by phone to any standard "terminal." Transmittals at 2-minute intervals alternate between a 7,300-ft coverage (shown here) and an expanded profile that covers only 2,200 ft. The expanded scale profiles are useful when low-level temperature structure is present.

The first four lines of data at the top describe conditions for each of the 2-minute subcycles that went into the average data plotted below. For example, for the first subcycle, the DOY (day of year) is Dec. 7; start time for the subcycle is 1615; precipitable water vapor was 0.99 cm; assumed vapor-weighted height for the vapor was 4,000 ft; liquid burden was 41 microns; etc. The set of five lines of data are observed brightness temperatures corresponding to each of the four subcycles and the average for the data period. The entries are observed brightness temperature corresponding to applicable heights of 120, 192, 334, 472, 690, 993, 1,380, 1,380, 1,890, 2,170, 2,530, 3,420, 3,420, 4,500, 5,100, 5,730, and 6,860 ft above the station.

Vapor comparisons with radiosondes were also very good: precipitable water vapor RMS of 0.064 cm (clear weather), and 0.16 cm (cloudy, rain, snow). More extensive studies will be made of alternative retrieval procedures, especially for stratus cloud conditions. The increased knowledge that this experience will produce can be applied directly to subsequent uses of the MARS system for the CARB.

4.6 REFERENCES

4-1 E. G. Njoku, Proc. IEEE, 70, 728 (1982).

4-2 A. H. Barrett and V. K. Chung, J. Geophys, Res., 67, 4259 (1962).

4-3 D. H. Staelin, J. Geophys. Res., 71, 2875 (1966).

4-4 N. E. Gaut, Tech. Rept. 467, Res. Lab. of Electronics, Massachusetts Institute of Technology, 101 pp. (1968).

4-5 M. L. Meeks and A. E. Lilley, J. Geophys. Res., 68, 1683 (1963).

4-6 W. B. Lenoir, Ph.D. Dissertation, Massachusetts Institute of Technology, (1965).

4-7 D. H. Staelin, P. W. Rosenkranz, F. T. Barath, E. J. Johnston, J. W. Waters, Science, 197, 991 (1977).

4-8 D. H. Staelin, A. H. Barrett, P. W. Rosenkranz, F. T. Barath, W. B. Lenoir, in "Nimbus 6 User's Guide," J. E. Sissala, ed. (NASA Goddard Space Flight Center, Greenbelt, MD, 1976), p. 59.

4-9 M. T. Decker, E. R. Westwater, F. O. Guirand, J. Applied Meteorology, 17, 1788 (1978).

4-10 B. L. Gary, Report 5030-498, Jet Propulsion Lab., Pasadena, CA (1981).

4-11 B. L. Gary, Final Report ESD3-0872, Jet Propulsion Lab., Pasadena, CA (1981).

4-12 B. L. Gary, (unpublished) EPA Proposal (1980).

APPENDIX A

JPL'S METEOROLOGY SUPPORT TO THE CALTECH ACID FOG FIELD MEASUREMENT PROJECT

B. L. Gary, June 25, 1982

JPL's MARS van was deployed on three days during the month of June in support of Caltech's acid fog measurement project. Caltech operated a pH sampler at Henninger Flats (2,630 ft MSL), while JPL measured vertical integrated contents of atmospheric water vapor and cloud liquid water at the Eaton Canyon Nature Center (970 ft MSL), located below the Caltech sampling site. The MARS van also made vertical temperature profile measurements, but these will not be discussed in this report.

Figure A-1 is a photograph of the MARS van. Only passive microwave radiometers are employed (no radar is used). The radiometer modules can be seen mounted on a platform at roof level in the photograph. Sky brightness temperature measurements are made at frequencies 22 GHz (water vapor), 31 GHz (liquid water), and 54.0, 55.3, and 57.5 GHz (oxygen molecules). The highest three frequencies are used to determine vertical temperature profiles. Elevation angle scanning is performed with 2-minute repeat times. All meteorology parameters are determined at this 2-minute interval. Retrieved parameters are displayed on a TV in real-time and raw data is recorded on magnetic tape cassettes for later playback and analysis.

Figures A-2 to A-4 are plots of liquid water cloud content (continuous line) and precipitable water vapor content (dot pattern). Considering Figure A-4 (June 22, 1982), which is the day of greatest interest, the cloud liquid water content varied from a high of 570 microns (at 10 to 11 a.m.) to about 100 microns (at 3:20 p.m.) At about 5 p.m., it was noted visually that the cloud layer had completely "burned off". The precipitable water vapor content remained fairly stable, at 1.7 cm (10 to 11 a.m.) to 2.0 cm (2 to 3 p.m.).

Cloud base estimates were made (visually) during the observing period on June 22, 1982. They varied from 700 ft (AGL) to 1,800 ft (AGL). Henninger Flats is at 1,660 ft (AGL), so the cloud base "rose" above the Caltech sampling site at about 2:30 p.m. The 1:30 p.m. radiosonde operated by SCE near Ontario showed that the cloud tops were at about 2,000 ft (AGL). With cloud top information (which should remain stable throughout the burnoff period) and cloud base information, it is possible to derive cloud thickness versus time. Since the MARS measures the vertical integral of liquid water throughout the cloud layer, and since we have estimates of cloud thickness, a simple division of one parameter by the other yields "liquid water content", LWC. This LWC [gm/m] determination is shown in the figures (near the top). For June 22, LWC varies from 0.60 to 0.86 during the 5-hour period during which Caltech pH measurements were taken. Between 2:30 p.m. and burn-off, LWC decreases to zero.

These LWC determinations are cloud layer averages. It is generally true that LWC decreases from a maximum value near the cloud tops to a zero value at the cloud base in a quasi-linear manner. It is interesting that on June 22, from 10 a.m. to 2:30 p.m., LWC remains constant while the thickness changes by a

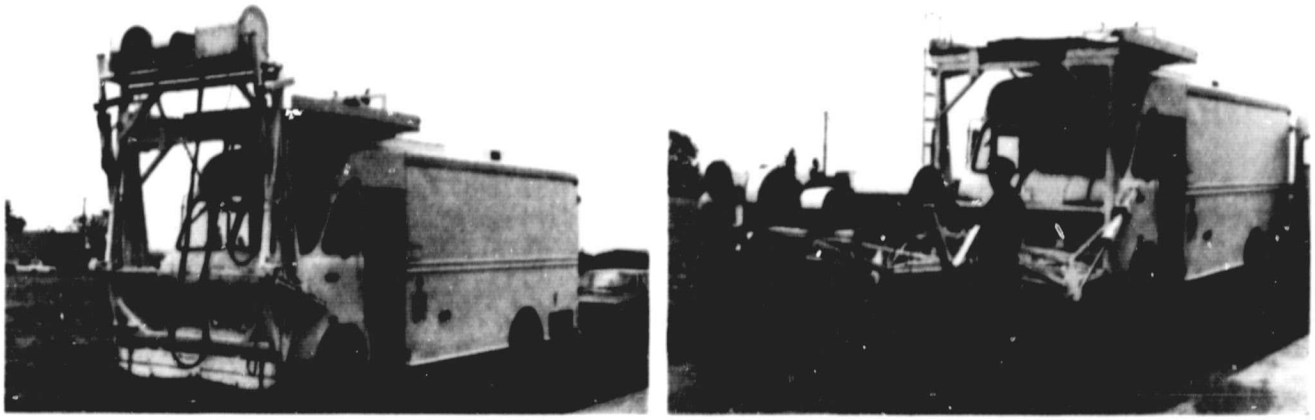

Figure A-1. MARS Van. This shows the mounting arrangement of the three radiometer units on a platform that is hydraulically lifted up for measurements (Right photo) and down, for servicing of the radiometers (Left photo). The large radiometer box, on the right, measures line-of-sight integrated water vapor and liquid water.

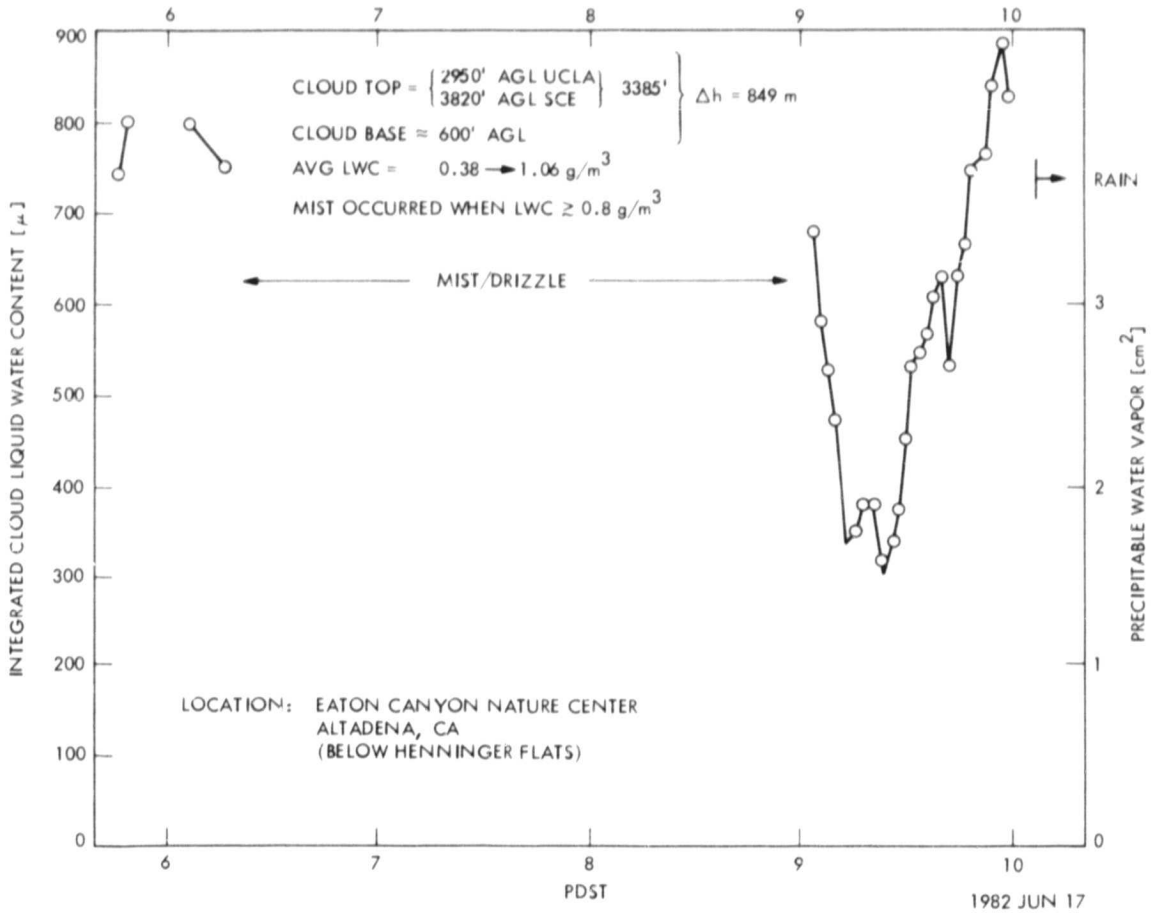

Figure A-2. Plot of Cloud Liquid Water Content Versus Time, During Acid Fog Coordinated Measurements with Caltech Investigators. Liquid content varies from 300 to 900 microns during this 4-hour period, during which there is no apparent "burn-off."

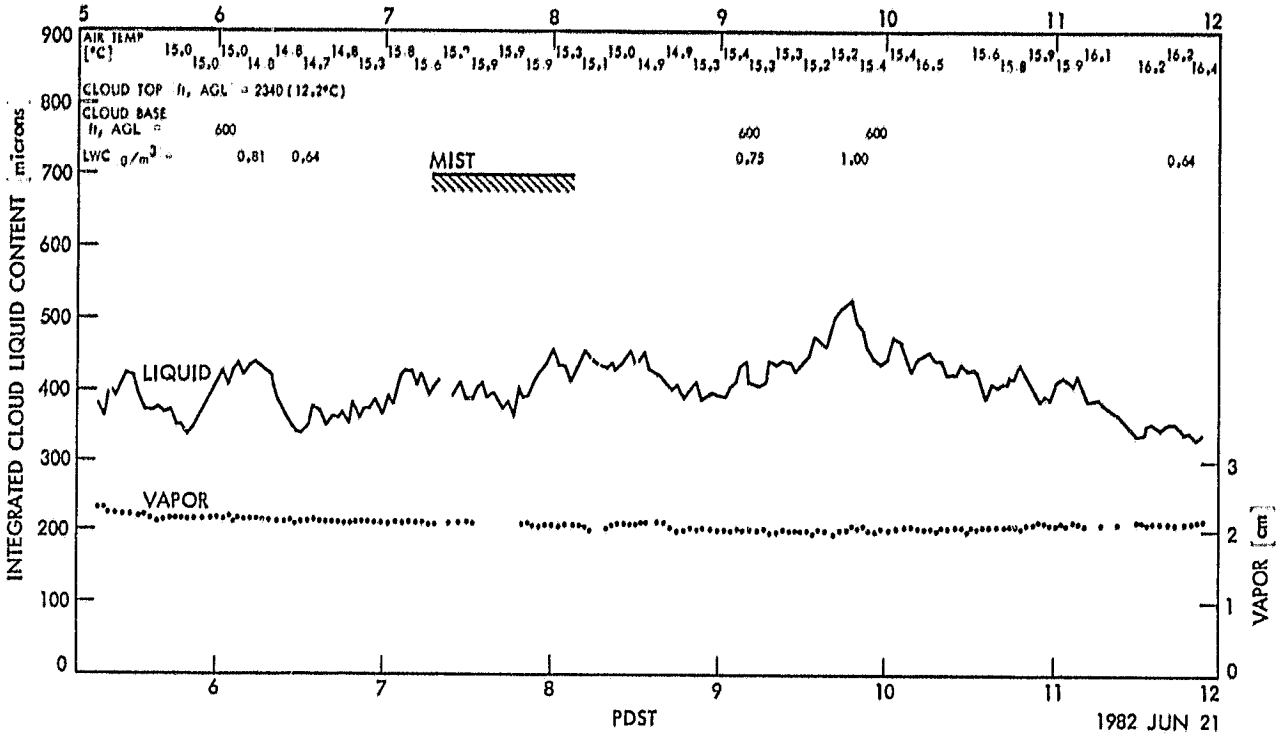

Figure A-3. Plot of Liquid Water (Connected Line) and Water Vapor (Dots) During Another Status Morning, During Which There is Also No Burn-off in Progress. Water vapor burden is steady, at about 2.1 cm. Cloud base and top altitudes are available, from which the liquid burden of about 400 microns can be converted to a cloud layer average "liquid water content," LWC, of 0.64 to 1.00 gm/m^3.

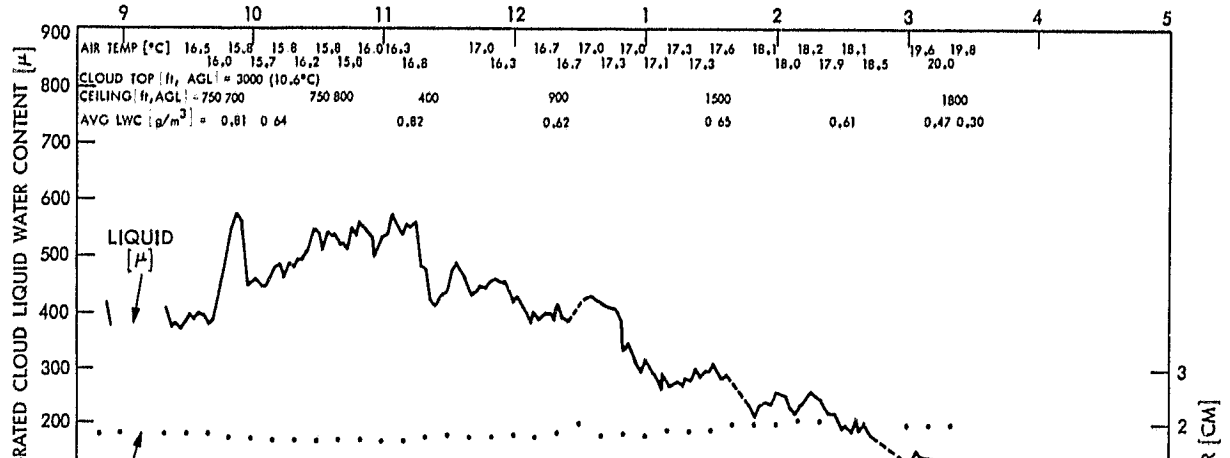

Figure A-4. Plots of Same Quantities as in Previous Figures, Except on this Date, the Stratus Layer Burned-off at the End of the Observing Period. LWC values are similar to those of the previous day (previous figure).

factor of two. This suggests that during burnoff, this cloud layer was eroding from the bottom in a way that left upper levels unaffected. We must also assume that LWC was approximately the same throughout the cloud layer (during this burnoff period). These inferences are uncertain and are offered here to suggest the kind of constraints that MARS data might be able to provide during the later phases of data analysis, when a qualified meteorologist will presumably provide interpretation guidance.

LWC information can be used for the interpretation of pH measurements. For a given amount of pollutant we can imagine smaller departures from pH 5.6 as LWC increases. The same dilluting principle applies here that accounts for better air quality for deeper mixed layers. The MARS generated LWC data should therefore be useful in modeling the Caltech measurements of pH.

Burnoff patterns differed for the three measurement periods at Eaton Canyon. Although June 21 and June 22 began with about 400 microns of LWC, burnoff was complete for only one of the days. Figure A-5 is a burnoff event that was recorded May 21 at SCE's Ontario radiosonde launch site (note the different liquid scale). This was a slow burnoff event, averaging about 40 microns per hour, versus 100 microns per hour for June 22.

The June 22 "outside air temperature" (OAT) changed very little before 1 p.m., during which time the LWC of the stratus clouds was 400 microns. The rise in OAT was 1°C/hr for LWC of 300 microns and 2°C/hr for LWC of approximately 190 microns. One June 21, with about 400 microns of stratus during the entire 6-hour observing period, OAT rose only 1.3°C, or at a rate of 0.2°C/hr.

Mist and drizzle appear to occur when LWC exceeded about 700 microns, on June 17. On June 21, a 50-minute period of mist occured without an associated rise in LWC, when LWC was a steady 400 microns. On June 22, no mist occured during a rise in LWC to 550 microns. About the only conclusions to be drawn from this are that: 1) mist can occur for LWC values as low as 400 microns (but has never been seen for lower values), and 2) mist can be absent for LWC values as high as 900 microns. This is to say that the "turn on" value for mist production is LWC of 400 to 900 microns, with the exact value determined by properties we weren't measuring.

Analysis of this data will continue, but this interim status report outlines the major results of the MARS van observations that were made in support of the Caltech acid fog project.

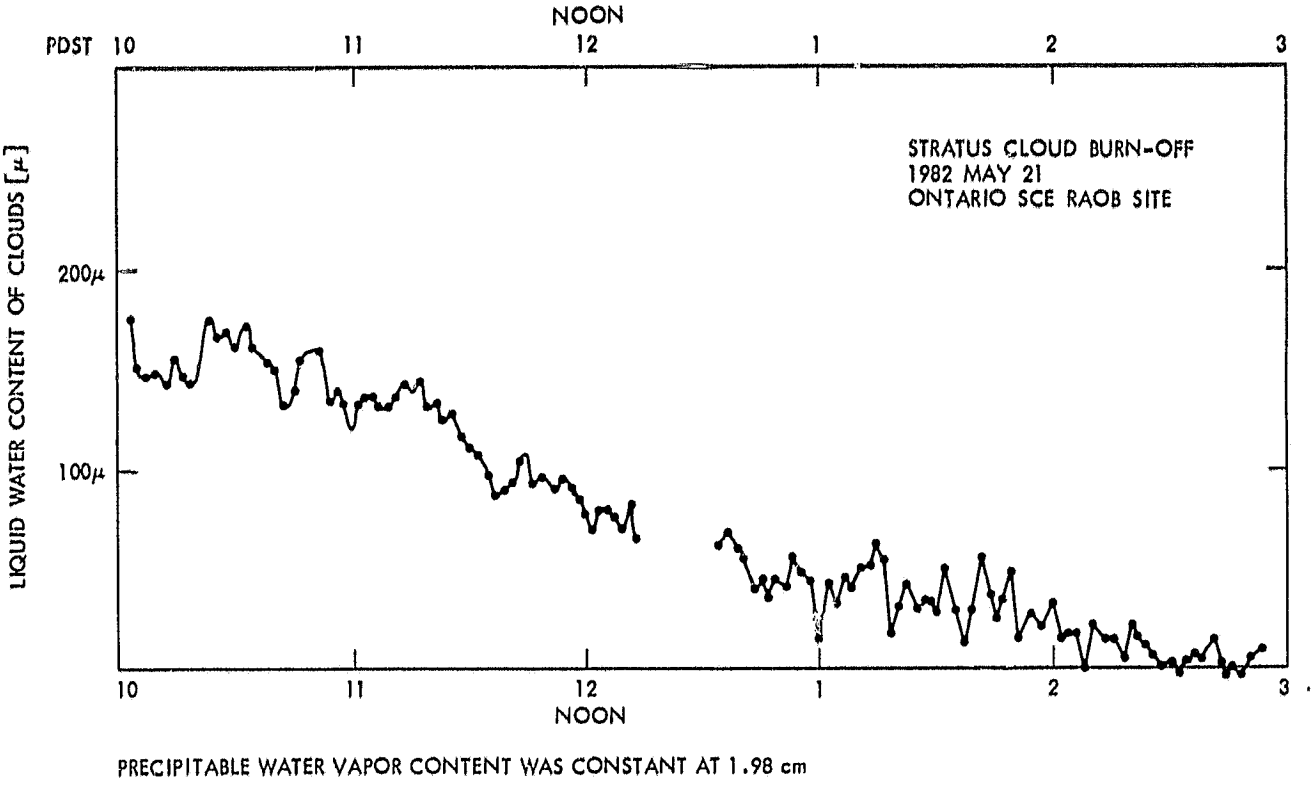

Figure A-5. Plot of Liquid Water Burden for Observations in May at the Southern California Edison Radiosonde Launch Site Near Ontario, CA. Burn-off proceeded very slowly and became more "erratic" near the end, signifying stronger convection cell activity.

APPENDIX B TEMPERATURE PROFILE RETRIEVAL CAPABILITIES USING MICROWAVE OBSERVABLES
Theoretical Limitations and Computer Simulations

Bruce L. Gary (NASA/JPL); December 1982

No temperature profile retrieval of physical properties from observables is unique. Figure B-1 shows two profiles that produce almost identical observables. Living in the real world of noisy observables, it can be said that if the observables are the same to within some noise-related criterion, then preference for one or the other of the profiles depicted in Figure B-1 cannot exist if we want to limit ourselves to just "agreement in observable space."

Having said that uniqueness does not exist, I shall now state that some of the "sister solutions" to the retrieved one (the dashed line) are only of academic interest. Common sense, or experience with atmospheric profiles, says that the short spatial wavelength oscillations (Figure B-1a) are "contrived," and can be ignored in practice. Thus, there is a category of non-unique solutions that "don't matter."

But there is also a category of non-unique solutions that do matter. These are most frequently the high altitude structures, such as subsidence inversions (Figure B-1b). The remainder of this discussion will relate to the situation of the "high altitude inversion layer" (HAIL).

The guiding principle determining when altitude structure is "lost" can be expressed most straightforwardly in terms of "averaging kernels." Figure B-2 represents an approximation of the MARS averaging kernels. The averaging kernel is defined in such a way that the retrieved temeprature is the "averaging kernel weighted average of the true temperature." Oscillations in T(h) structure are lost whenever the altitude wavelength of the oscillations is short compared with the width of the averaging kernel. Hence, it is always possible to "superimpose" short wavelength oscillations upon an otherwise obtained retrieved profile, and still retain compatibility with the observables. Since a HAIL contains components of such short wavelength oscillations, some of the HAIL structure will be "invisible", and may therefore be lost in the retrieval process. All long wavelength components of the true temperature profile will be "captured" during the retrieval process. Hence, these long wavelength components of HAIL will be represented in the retrieval. For such long wavelength components to be present, we require one of two conditions: 1) the temperature contrast across the inversion layer must be large; or 2) the inversion layer must be at a low altitude (where short altitude wavelengths can be "caught" due to the shallow width of the averaging kernels at these low altitudes).

Thus, there are two types of HAIL: those that can be "caught" (represented in the retrieval), and those that are "lost" (not represented in the retrieval). Figure B-3 illustrates examples of these two types. These remarks apply to the deterministic retrieval algorithm (i.e., Backus-Gilbert), to the statistical retrieval algorithm type, and to the least squares types of retrieval algorithms. The reason it applies to all these retrieval types has to do with very basic concepts of "information content" of the observables.

Before discussing the HAIL situation further, I want to survey the temperature profile types, in a very general way, and indicate which ones are easy or hard to retrieve. Figure B-4 summarizes the categories of profile shape that

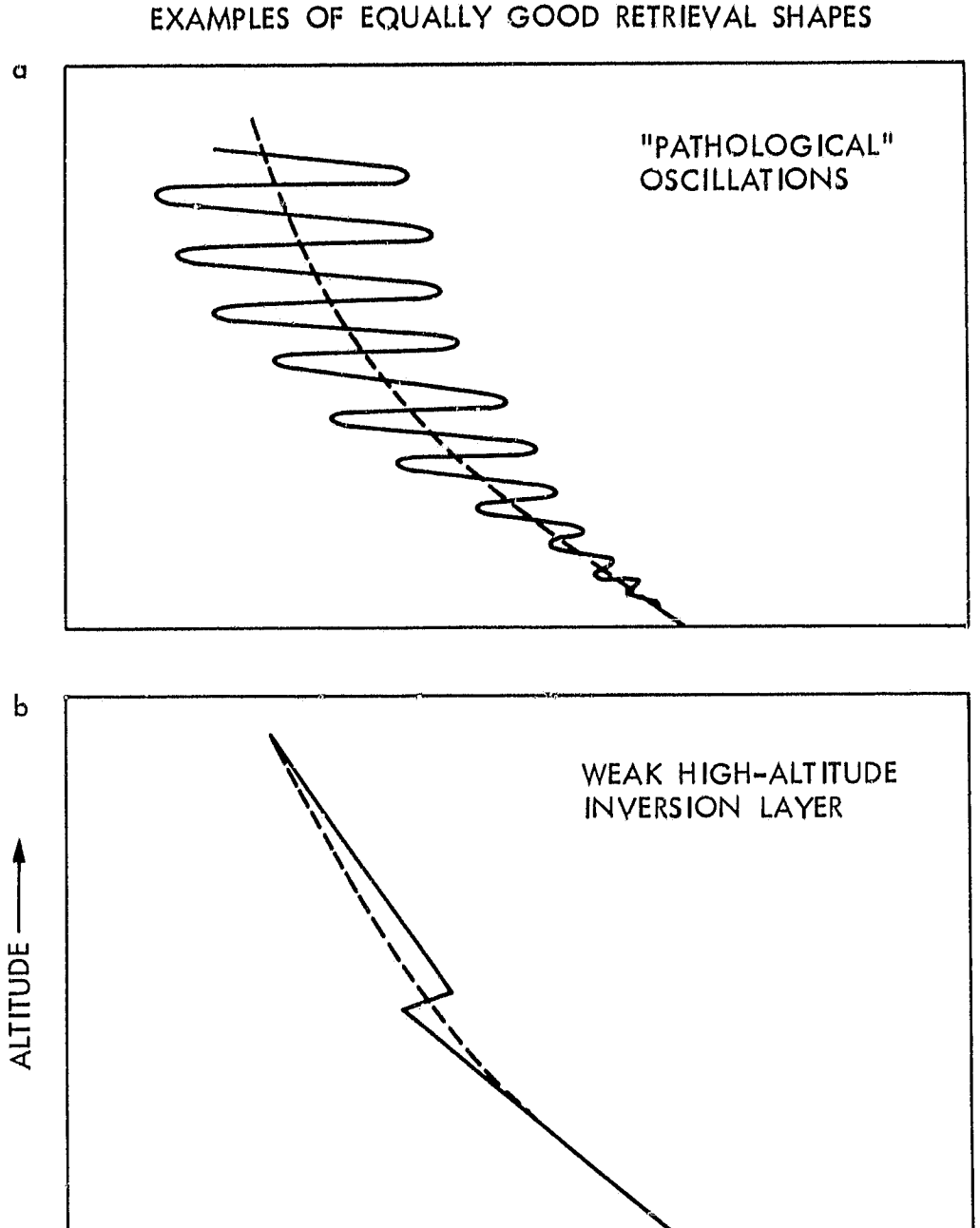

Figure B-1. Both Panels Illustrate Types of Altitude Temperature Profiles That Are Difficult to Retrieve Using Microwave Observables

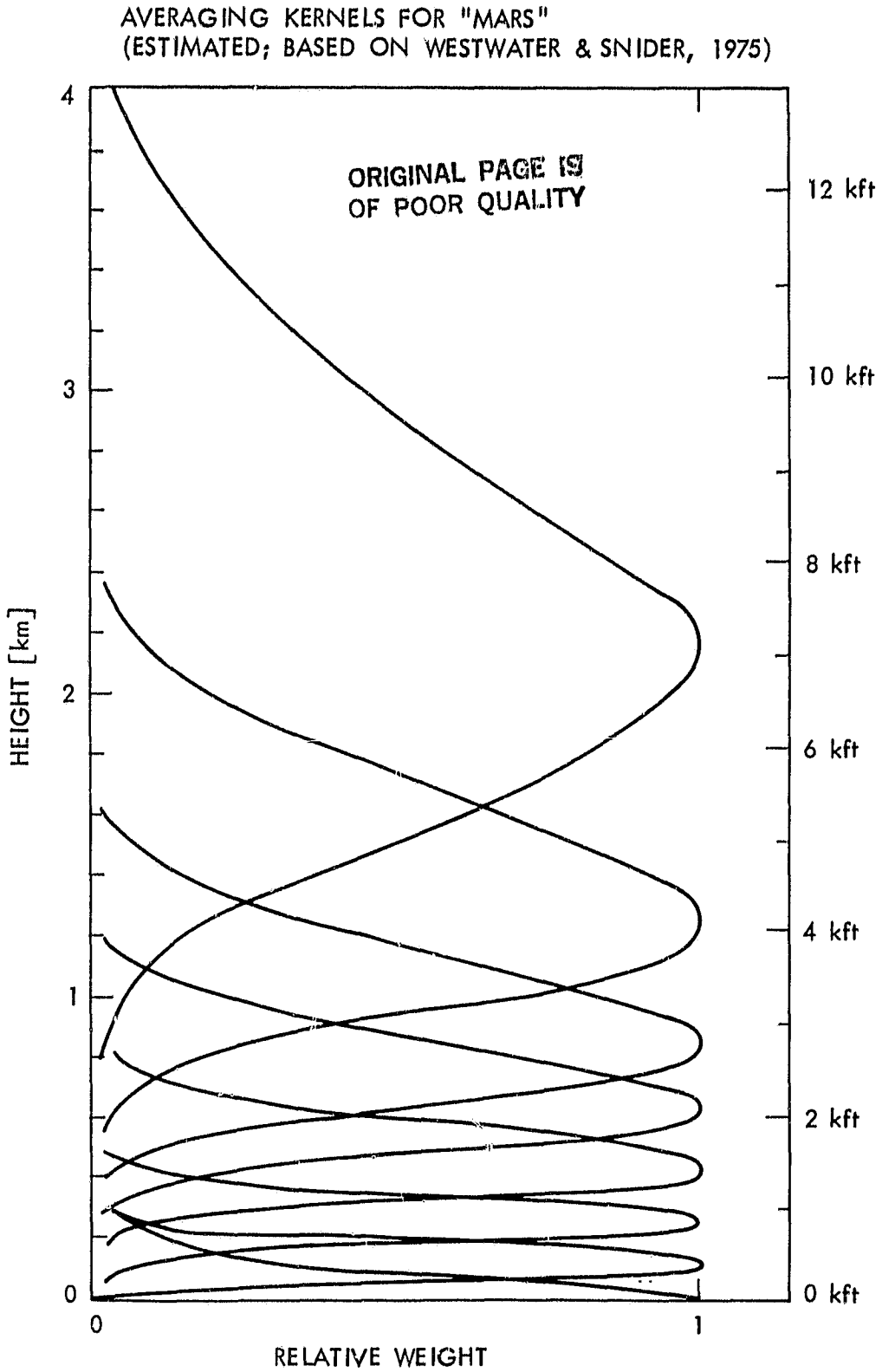

Figure B-2. These Are Estimated "Averaging Kernels" That Apply to the MARS System. A MARS-retrieved air temperature for the altitude 4,000 ft, for example, would actually be an average temperature, with the weighting given by the averaging kernel that "centers" on the 4,000 ft altitude. Averaging kernels for altitudes that are intermediate to those shown also exist.

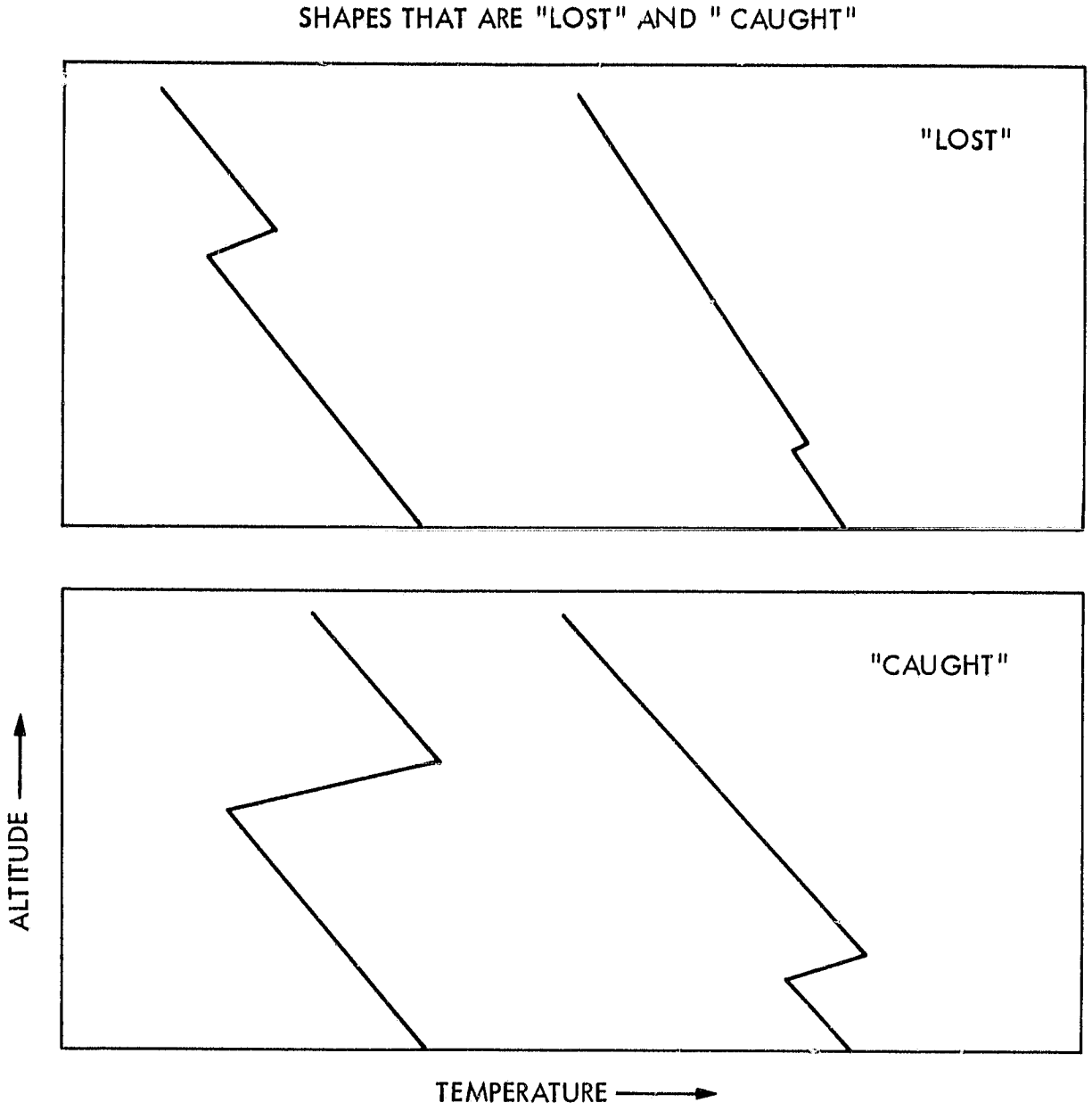

Figure B-3. Shapes That Are "Lost" and "Caught." Upper panel profiles are likely to be retrieved as smooth trace profiles, because the inversion structure is either too high in altitude or is too small in temperature contrast. Structure in the lower panel, however, would be represented in the retrieval, by the same reasoning.

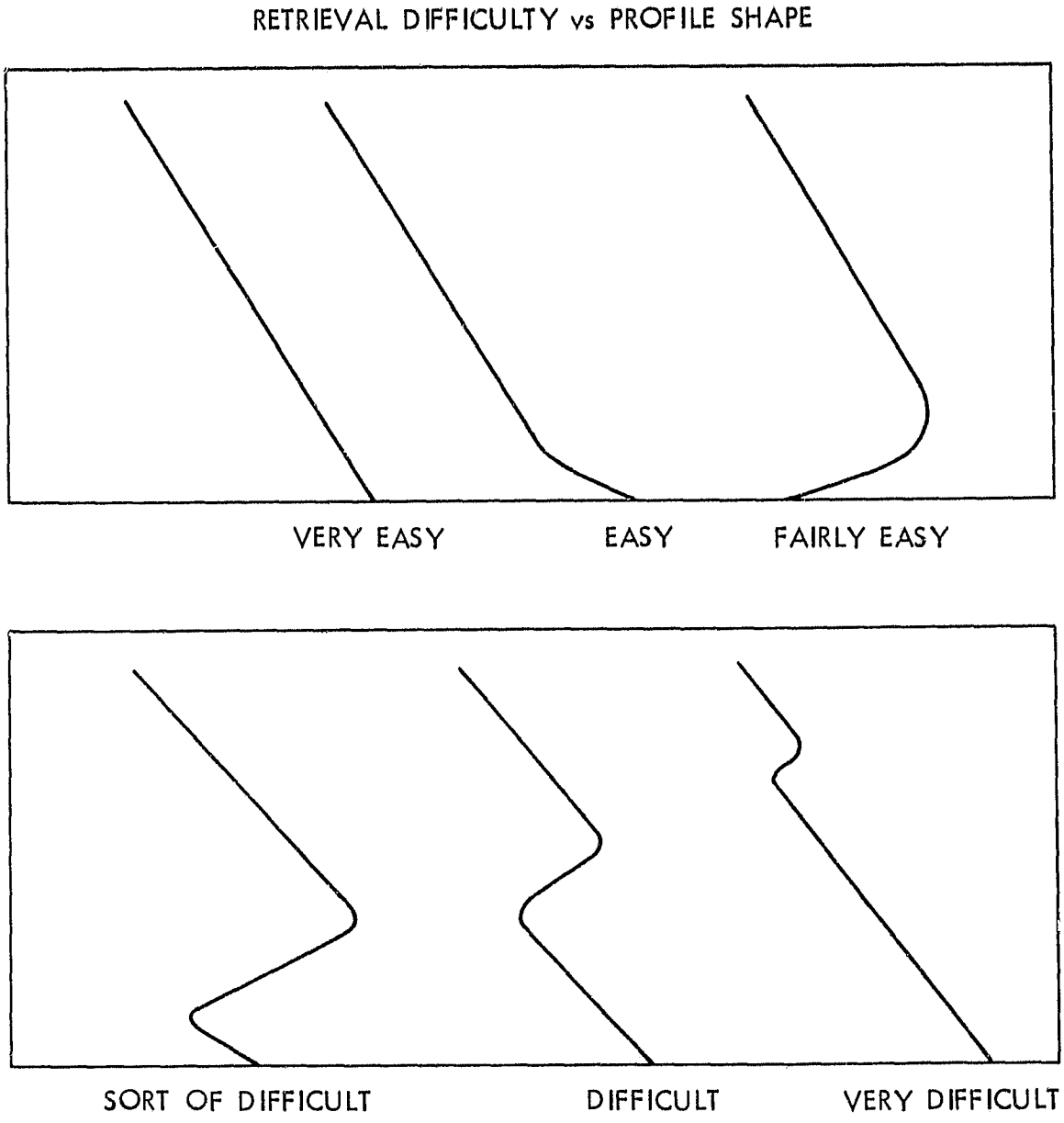

Figure B-4. Retrieval Difficulty vs. Profile Shape. Altitude temperature profile shapes can be classified according to the expected closeness between retrieved profile and acutal profile (in some RMS-difference sense). This figure summarizes the shape types in terms of "ease" of retrieval.

are commonly encountered in real life situations. The profile shapes are arranged in order of increasing retrieval difficulty. The rationale for this particular sequence of shapes can be generated by the reader using the concepts just described. That is, "structure" at low altitudes can be "caught" because of the good altitude resolution (of averaging kernels) near the surface, while structure at higher altitudes is "lost" due to the greater amount of altitude averaging that occurs there.

Our field experience with MARS provides confirmation of the relative ease of retrieving the shapes depicted in Figure B-4. Straight line (adiabatic) profiles are very easy; and even the magnitude of the lapse rate is observed to be correct for these retrievals. Surface-based superadiabatic layer profiles are retrieved with ease. And ground-based inversions are retrieved quite well. Low altitude IL profiles can be seen in the data, although their temperature contrasts tend to be under-represented. Figure B-5 shows a sequence of "observed" and true profiles. The "observed" are "raw data," or observed "brightness temperatures" plotted at their "applicable heights" (in other words, these raw data plots haven't undergone the structure-enhancing retrieval process). Note the agreement for straight line and ground-based profiles. Even the elevated inversion appears in the observed data, though with a smaller temperature contrast (due to the absence of undergoing any retrieval process). Figure B-6 summarizes the three particular field observation evaluation (in Ohio, in 1980). What's missing in our field measurement experience, so far, are encounters with HAIL! Until these high altitude IL's are encountered, we cannot "prove" how well our retrieval of them will work.

Computer simulations, however, can be performed to show how well MARS observables should translate to HAIL detection. This has already been done. The results are very encouraging! Figure B-7 shows the results of a simulation for ILs at 3,000 ft and 700 ft (HAIL and low-altitude IL, respectively). The HAIL retrieval shows the presence of an IL at an altitude that is approximately correct, although the magnitude of the potential temperature contrast across the IL is under-estimated. If mixing depth were the desired parameter to retrieve, then the retrieved and true mixing depths would agree. The low-altitude IL is dramatic in accuracy! This is an actual temperature profile (occuring at El Monte in June 1977). Such high temperature contrasts across the IL are uncommon. This computer simulation of "noisy" MARS observables suggests that the goal of measuring low-altitude IL structure is do-able, and the goal of measuring HAIL is also sometimes do-able. A continuum of difficulty exists, and Figure B-7 provides a "feeling" for where the edge of do-ability is located.

A crucial question for the CARB is: "Will MARS produce the IL/mixing depth information that is needed during a smog alert?" To answer this, we must recognize that smog alerts are associated with meteorological conditions of: 1) low-altitude IL; 2) high temperature contrast across the IL; and 3) stagnant air (low wind speed). In other words, HAIL is not associated with smog alerts! Figure B-8 is an example of smog alert temperature profiles. These are profiles based on Los Angeles Airport soundings, and they are for the famous September 1979 ozone episode. The dotted plots are the radiosonde-measured early morning profiles, and the solid lines are estimates corresponding to late morning. These are definitely "low-altitude/high temperature contrast" profiles (not HAIL). It is likely that MARS would have done a good job in retrieving the mixing depth/IL properties that were needed for formulating and updating the smog alerts during this period.

COMPARISION OF ALTITUDE TEMPERATURE PROFILES GENERATED BY THE PASSIVE MICROWAVE SYSTEM (LINES) WITH TETHERSONDE DATA (CIRCLES)

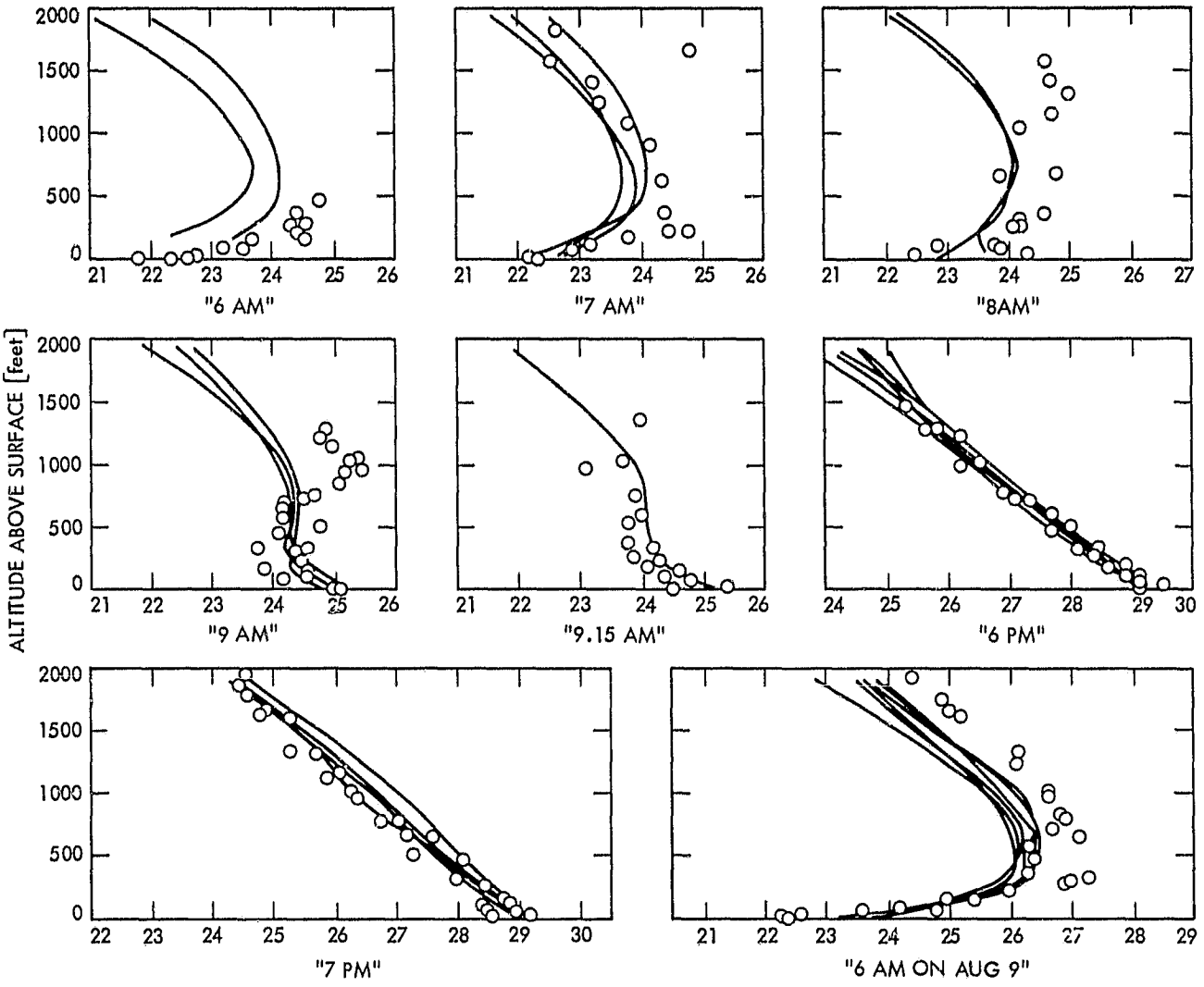

Figure B-5. MARS Altitude-Temperature Profiles (Lines) Are Compared with Tethersonde-Derived Profiles (Circles). The data is from an EPA-funded measurement program in Croton, Ohio, in 1980. The two profiles agree best for straight line profiles, agree pretty well for ground-based inversions, and agree least for elevated inversions.

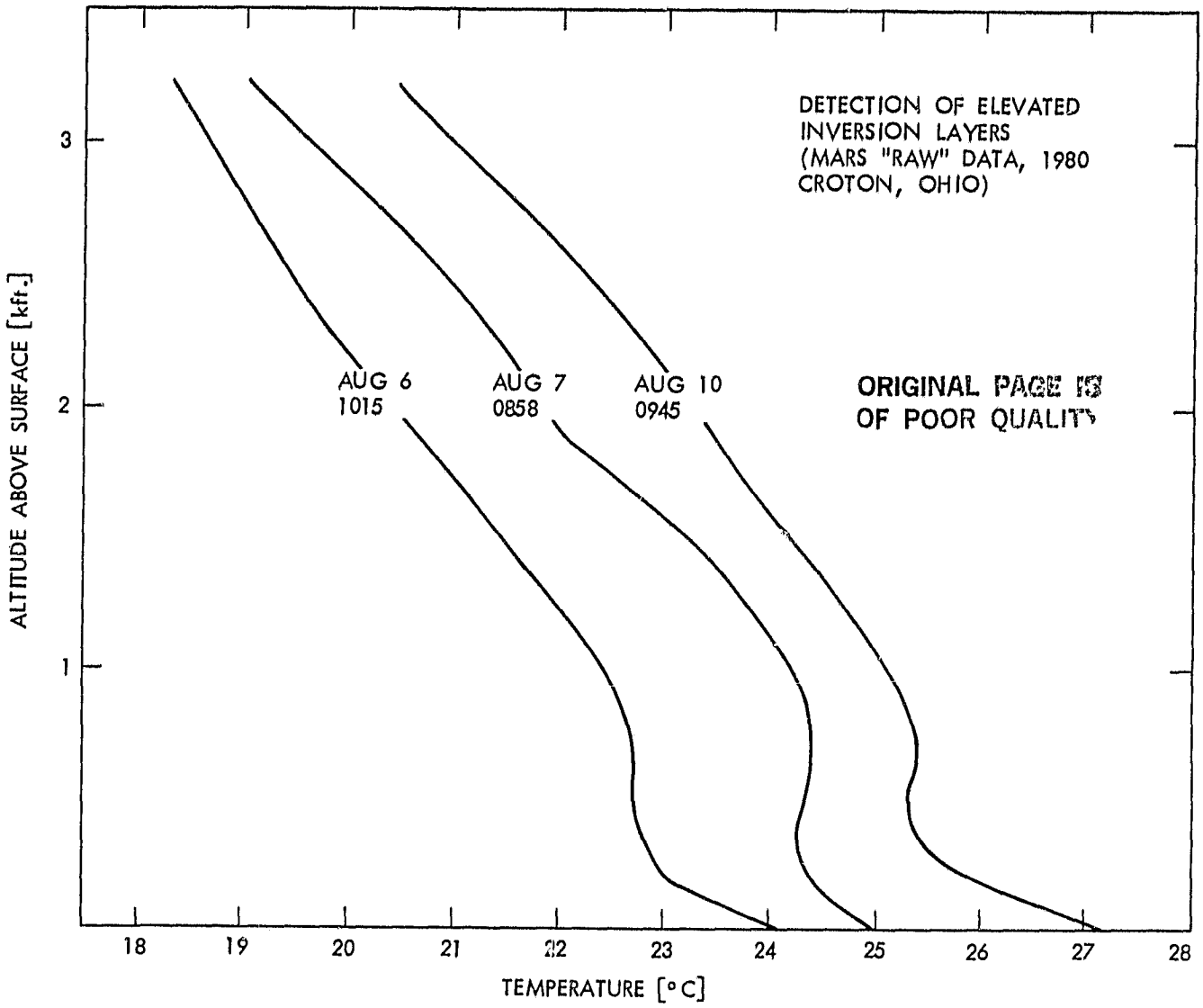

Figure B-6. Samples of Three MARS Profiles During Morning Periods When Elevated Inversion Layers Were Present. The early-morning ground-based inversions were converting to late-morning adiabatic lapse rate profiles. From such "raw data" plots is is apparent that inversion structures were present, and the altitudes of the bases and tops can easily be estimated. Note the small temperature contrast.

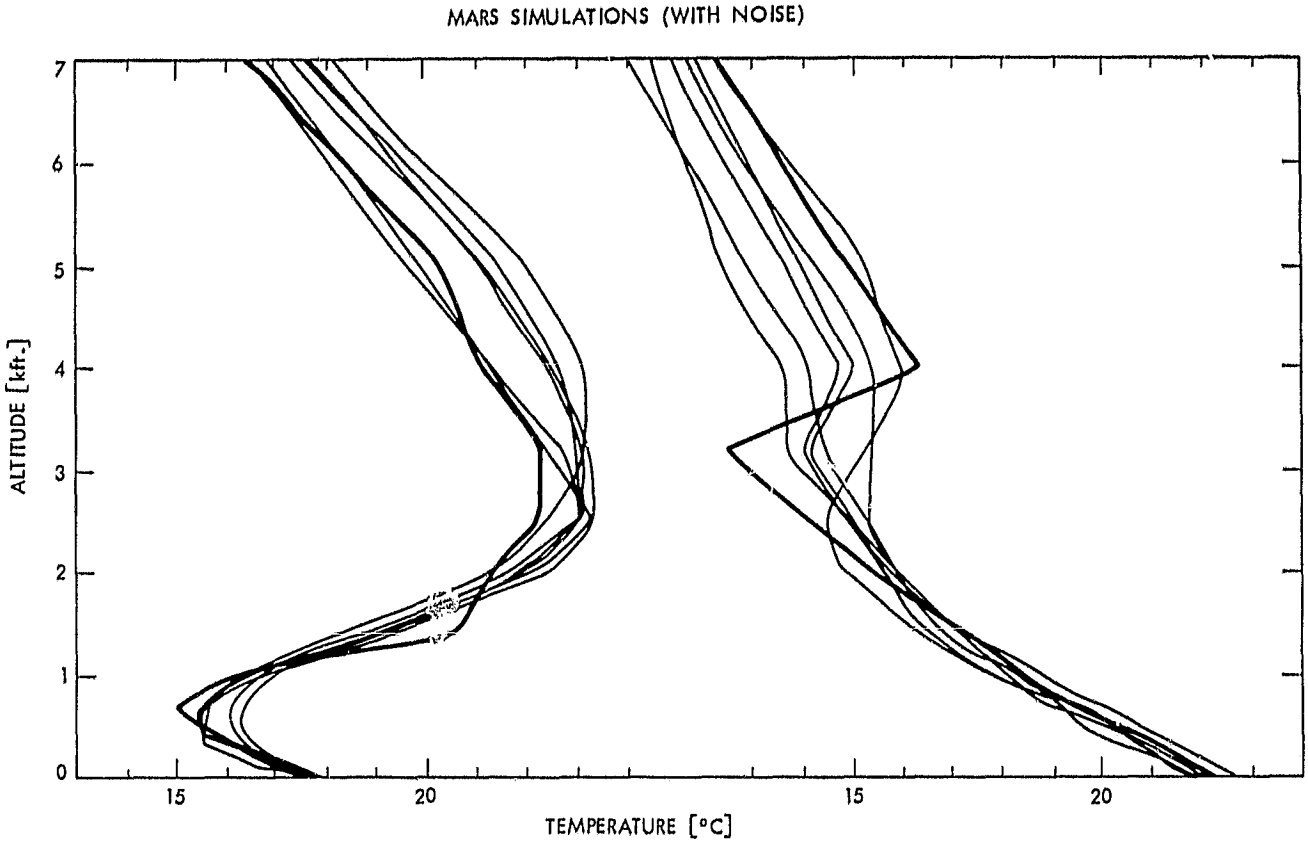

Figure B-7. Computer Simulations of MARS Observables with Noise. These simulations show that MARS observables contain sufficient information to permit retrieval of low-altitude inversion structure when the inversion layer has temperature contrasts of several ^{o}C (at altitudes of only a few thousand feet). The heavy line is "true" and the several thin lines are simulated retrievals, where each retrieval corresponds to a Monte Ca lo representation of stochastic measurement noise.

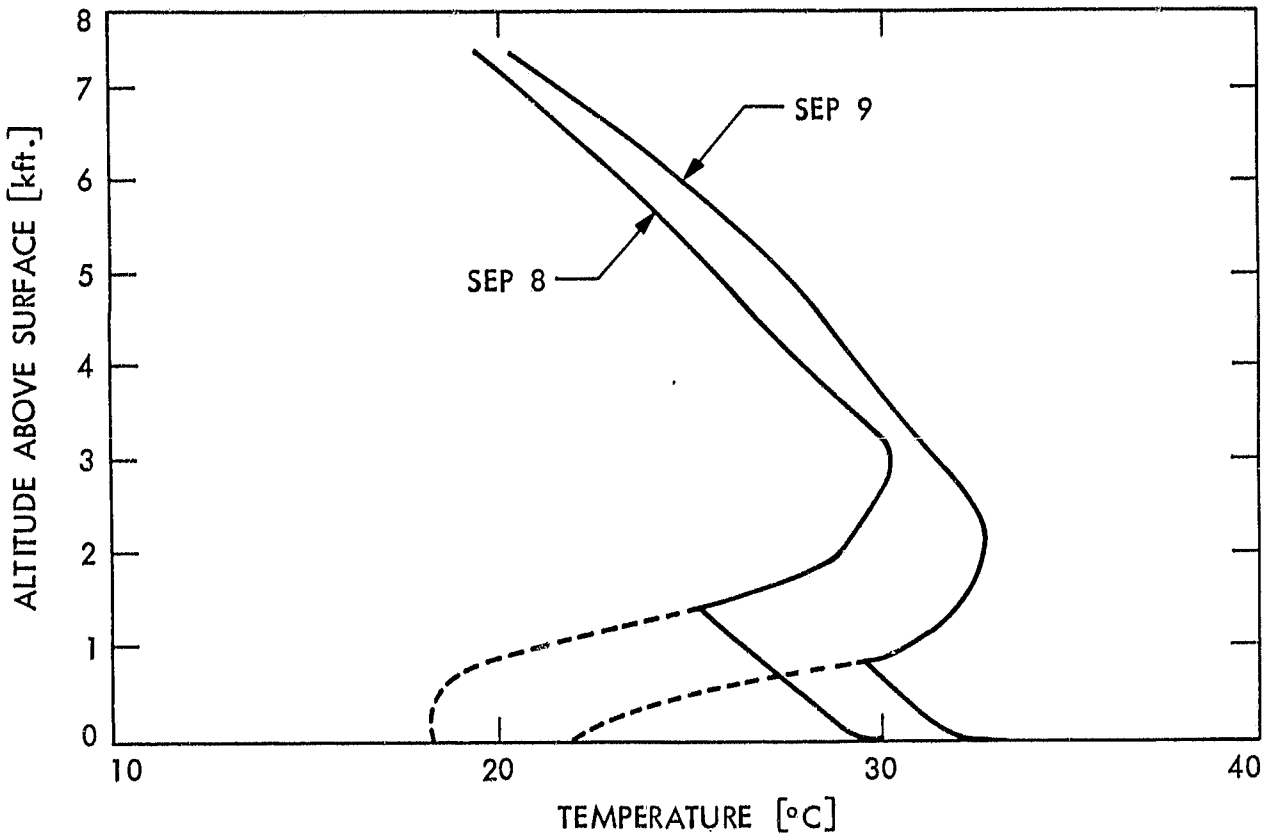

Figure B-8. Temperature Profiles During the Famous September 1979 Ozone Episode